Environmental Science
Processes & Impacts

Co-encapsulation of slow release compounds and *Rhodococcus rhodochrous* ATCC 21198 in gellan gum beads to promote the long-term aerobic cometabolic transformation of 1,1,1-trichloroethane, *cis*-1,2-dichloroethene and 1,4-dioxane

Journal:	*Environmental Science: Processes & Impacts*
Manuscript ID	EM-ART-12-2019-000607.R1
Article Type:	Paper

Co-encapsulation of slow release compounds and *Rhodococcus rhodochrous* ATCC 21198 in gellan gum beads to promote the long-term aerobic cometabolic transformation of 1,1,1-trichloroethane, *cis*-1,2-dichloroethene and 1,4-dioxane

Mitchell T. Rasmussen[a], Alyssa M. Saito[a], Michael R. Hyman[b] and Lewis Semprini[a]

[a]School of Chemical, Biological, and Environmental Engineering, Oregon State University, Corvallis Oregon, 97331 USA

[b]Department of Plant and Microbial Biology, North Carolina State University, Raleigh, North Carolina 27695, USA

Corresponding Author and address

Lewis Semprini

School of Chemical, Biological, and Environmental Engineering

Oregon State University

Corvallis, Oregon 97331

USA

E-mail Address: lewis.semprini@oregonstate.edu

Tel: 1-541-737-6895

Keywords

Cometabolism, co-encapsulation, gellan gum, TBOS and T_2BOS, hydrolysis, 1,4-dioxane, chlorinated aliphatic hydrocarbons; permeable reactive barriers

Environmental Significance

Aerobic cometabolism is an environmental process that has been utilized for the in-situ bioremediation of subsurface contamination with chlorinated aliphatic hydrocarbons and emerging contaminants, such as 1,4-dioxane. The process usually involves the addition of growth substrates, such as methane or propane, to promote the growth of microorganisms that express oxygenase enzymes that can oxidize contaminants. One drawback of this approach is the inhibition that results from the growth substrate and the contaminants competing for the same enzyme. Presented here is novel approach where passive long-term cometabolic treatment can be achieved by co-encapsulating in a gellan gum hydrogel a pure bacterial culture and a slow release compound that hydrolyses to produce a growth-supporting substrate. Contaminants diffuse into the hydrogel to be cometabolized. *Rhodococcus rhodochrous* ATCC 21198 (strain ATCC 21198) was successfully co-encapsulated in gellan gum beads with orthosilicates as slow release compounds (SRCs) that hydrolyze to produce 1- and 2-butanol. Effective transformation of a mixture of 1,1,1-TCA, *cis*-DCE and 1,4-D was achieved in batch reactors containing the beads. The beads can potentially be used to create a biological permeable reactive barrier for the in-situ treatment of chlorinated aliphatic hydrocarbons and emerging contaminants, such as 1,4-dioxane.

Abstract

Rhodococcus rhodochrous ATCC 21198 (strain ATCC 21198) was successfully co-encapsulated in gellan gum beads with orthosilicates as slow release compounds (SRCs) to support aerobic cometabolism of a mixture of 1,1,1-trichloroethane (1,1,1-TCA), *cis*-dichloroethylene (*cis*-DCE), and 1,4-dioxane (1,4-D) at aqueous concentrations ranging from 250 to 1000 µg/L. Oxygen (O_2) consumption and carbon dioxide (CO_2) production showed the co-encapsulated cells utilized the alcohols that were released from the co-encapsulated SRCs. Two model SRCs, tetrabutylorthosilicate (TBOS) and tetra-s-butylorthosilicate (T_2BOS), which hydrolyze to produce 1- and 2- butanol, respectively, were encapsulated in gellan gum (GG) at mass loadings as high as 10% (w/w), along with strain ATCC 21198. In the GG encapsulated beads, TBOS hydrolyzed 27 times faster than T_2BOS and rates were ~4 times higher in suspension than when encapsulated. In biologically active reactors, the co-encapsulated strain ATCC 21198 effectively utilized the SRC hydrolysis products (1- and 2-butanol) and cometabolized repeated additions of a mixture of 1,1,1-TCA, *cis*-DCE, and 1,4-D for over 300 days. The transformation followed pseudo-first-order kinetics. Vinyl chloride (VC) and 1,1-dichloroethene (1,1-DCE) were also transformed in the reactors. In the long-term treatment, the batch reactors with T_2BOS GG beads achieved similar transformation rates, but at much lower O_2 consumption rates than those with TBOS. The results demonstrate that the co-encapsulation technology can be a passive method for the cometabolic treatment of dilute groundwater plumes.

1. Introduction

Groundwater contamination with volatile organic compounds (VOCs) is a widespread issue throughout the United States.[1,2] Over 50% of more than 3500 groundwater samples collected from 98 major drinking water supply aquifers from 1985-2001 contained at least one anthropogenic contaminant with VOCs detected most frequently.[2] Among the top 15 VOCs detected in this survey, eight were chlorinated aliphatic hydrocarbons (CAH); chloroform (CF), perchloroethylene (PCE), trichloroethylene (TCE), 1,1,1-trichloroethane (1,1,1-TCA), *cis*-1,2-dichloroethylene (*cis-DCE*), *trans*-1,2-dichloroethylene (*trans*-DCE), dichloromethane (DCM), and 1,1-dichloroethane (1,1-DCA). All of these CAHs are listed by the Center for Disease Control (CDC) as being likely human carcinogens as well as having other harmful environmental and human health concerns.[3] Of increasing concern is the high likelihood for CAH plumes

to contain multiple CAHs as well as co-contaminants, such as 1,4-dioxane (1,4-D), which is also listed as a likely human carcinogen.[4] 1,4-D was most commonly used as a chemical stabilizer for chlorinated solvents, mainly 1,1,1-TCA to prevent decomposition due to reactions from light, heat, oxygen, or acid-base chemistry;[4,5] 1,1,1-TCA formulas contain up to 2% - 8% by volume 1,4-D.[5,6] 1,4-D is a commonly detected groundwater contaminant in areas with chlorinated solvent contamination.[6,7] Of over 2000 sites evaluated in California, 194 contained 1,4-D, 95% of sites had at least one chlorinated solvent, and 76% had both 1,4-D and 1,1,1-TCA present. The median value of the range of maximal historical 1,4-D concentrations at these sites was 365 µg/L.[8]

The ubiquitous and long-term contamination of groundwater has allowed CAHs and co-contaminants to diffuse into saturated low permeability zones, such as clay layers, within aquifers.[9] Common remediation techniques, such as pump-and-treat and soil vapor extraction, are less effective at treating compounds within low permeability zones due to diffusion limitations and inability to remove or target the contaminant directly.[10] Also, current active remediation techniques often require long-term site occupation, are not economical, and are not capable or are ill-equipped for the treatment of mixtures of contaminants that have varying physical and chemical properties. These issues emphasize the need for exploration into long-term passive and economical remediation techniques such as bioremediation. 1,4-D, is fully miscible in water (infinitely soluble) and has a low octanol water partition coefficient (K_{ow}).[4,5] 1,4-D is also generally resistant to anaerobic transformation.[11] These chemical characteristics result in 1,4-D having a high mobility in groundwater with the potential to form extended dissolved plumes.[12] 1,4-dioxane is not effectively removed by air stripping or sorption onto activated carbon, which is commonly used for the ex-situ treatment of CAHs.

With the exception of PCE, all listed CAHs above as well as 1,4-D have the potential to be cometabolically transformed in-situ by aerobic microorganisms.[12–15] Aerobic cometabolism is a process were microbes utilize a primary growth substrate for cellular growth and energy, and fortuitous degradation of contaminants occurs due to the expression of specific enzyme systems within active microbes.[13,16] This study focused on the bacterium *Rhodococcus rhodochrous* ATCC 21198 (strain ATCC 21198) which has been shown to be capable of aerobic cometabolic transformation of a wide variety of CAHs and common co-contaminants such as 1,4-D.[17–19]

Current bioremediation technologies for the remediation of mixtures of CAHs and 1,4-D have relied on the biostimulation of native microbes capable of aerobic cometabolism using propane as a primary substrate, or bioaugmentation and then stimulation with propane.[20,21] Though biostimulation with gaseous substrates, like propane, has been successful at generating biomass capable of transformation and mineralization of CAHs in-situ, there are concerns related to explosion hazards as well as the lack of

sustainability due to the need for long-term site occupation for continuous injection of gaseous substrates to sustain populations of cometabolically active microbes.[13,16,22,23]

Passive treatment systems, such as permeable reactive barriers, have the potential to reduce costs and eliminate the need to extract groundwater or continuously add substrates, electron acceptors, and nutrients for biological treatment. Scherer et al. (2008)[24] provides a review of permeable reactive barriers for groundwater treatment using chemical and biological methods. Upadhyay and Sinha (2018)[25] review permeable reactive bio-barriers (PRBBS) for environmental clean-up. For aerobic treatment, barriers have focused on contaminants that can be metabolized, such as BTEX, through the addition of slow release forms of O_2-releasing compounds (ORCs) such as calcium or magnesium peroxides. However, there has been little attention given to the development of PRBBS for aerobic cometabolism. Reported here is a novel system that was developed to promote long-term passive aerobic cometabolism that might be used to construct PRBBS.

The passive cometabolic system developed here involves encapsulating a pure microbial culture in a hydrogel along with a slow release compound (SRC) that hydrolyze to produce an alcohol. The released alcohol maintains the activity of the co-encapsulated microorganisms and enables sustained cometabolic degradation of contaminants, which diffuse into the hydrogel. Natural hydrogel matrices such as alginate, agar, and agarose have been used to physically buffer microbes from environmental conditions by providing a diffusion layer that decreases toxic levels of ambient compounds, retards any changes in chemical and temperature conditions, and protects from predation by protozoa.[26–28] Encapsulation has also been investigated for its ability to inhibit the production of biofilms, which may reduce well clogging and increase the transport distance of cells through aquifer material.[27,29] Also, by controlling bead size, encapsulation may provide a control for bead affixation to aquifer material around low permeability zones.[29] Encapsulation for resting cell TCE cometabolism has also been reported.[30]

Gellan gum (GG) was used here to encapsulate strain ATCC 21198 with the SRCs, TBOS and T_2BOS. Gellan gum is natural gelling polysaccharide produced primarily by bacterium *Sphingomonas elodea*. It consists of chains of glucose, glucuronic acid, and rhamnose molecules[31,32] and similar to alginate, gelation of GG occurs via ionic crosslinking. Though GG gelation is ionically activated, the gelation process is more similar to the thermal hysteresis type gelation of agar and agarose.[33,34] GG gelation temperatures are dependent on the type and concentration of crosslinking cations, concentration of GG, and concentration of chelating agents.[31,34,35] Gellan gum has become a widely used hydrogel matrix replacing matrices like agar and alginate because it has superior rheological properties, chemical stability, temperature resistance and enzyme resistance.[31,33,35]

The cometabolic transformation of 1,4-D has been reported on a range of substrates for growth and or/induction of cometabolic enzymes as reviewed by Zhang et al. (2017)[36] and McElroy et al. (2019)[11]. Rolston et al. (2019)[19] recently reported the cometabolic transformation of 1,4-D by strain ATCC 21198 in microcosms fed with isobutane as a primary substrate. Strain ATCC 21198, is a soil-isolated microbe that expresses a short chain alkane monooxygenase (SCAM) capable of transforming 1,4-D. When grown on isobutane, strain ATCC 21198 rapidly cometabolically transforms 1,4-D at pseudo-first-order rates to low concentrations of ~1 ppb.[19] This strain can also cometabolically transform a broad range of CAHs including: 1,1,1-TCA, 1,1,2-trichloroethane (1,1,2-TCA), 1,2-dichloroethane (1,2-DCA), 1,1-DCA and chlorinated ethenes including: *cis*-DCE, 1,1-dichloroethene (1,1-DCE) and vinyl chloride (VC).[17,18,37] Mixtures of 1,4-D, 1,1,1-TCA , 1,1-DCE and 1,2-DCA are also effectively transformed by this strain.[18]

The novel process investigated here was to co-encapsulate active microbial cells with a large molecular weight SRC that hydrolyzes to produce an organic electron donor that can support cometabolism. The SRCs encapsulated with strain ATCC 21198 in this study were silicon-based organic compounds known as tetra-alkoxysilanes. These compounds consist of a central silicon atom bound via ester linkages to four alkoxy groups that can vary in carbon chain length and structure. Examples of these compounds used in this study include tetrabutylorthosilicate (TBOS) and tetra-s-butylorthosilicate (T_2BOS). While tetra-alkoxysilanes are insoluble in water at room temperature,[38] their ester bonds hydrolyze abiotically at varying rates which are determined by the pH of solution and the size or structure of the leaving group.[38–40] For example, TBOS hydrolyzes and releases 1-butanol while T_2BOS hydrolyzes more slowly and releases 2-butanol. The hydrolysis reaction can therefore be used to continuously generate alcohols over extended time periods.

While most studies of cometabolic biotransformations have focused on reactions involving unoxidized primary substrates such as methane, propane, or butanes, several studies have described aerobic cometabolic reactions supported by alcohols. For example, Semprini and Varcheeswaran (2002)[41] described a mixed culture grown on 1-butanol produced from TBOS hydrolysis that could cometabolically oxidize TCE and *cis*-DCE.[40] Previous studies with *Mycobacterium vaccae* JOB5 have shown that this strain can biodegrade 1,4-D [15] and MTBE [42] after growth on either 1- or 2-propanol. Hand *et al*. (2015)[15] also reported *Mycobacterium vaccae* JOB5 and *Rhodoccoccus* RHA1 can oxidize 1,4-D and TCE when grown on 1-butanol and strain ATCC 21198 has also been reported to oxidize VC after growth on isopropanol.[43] The potential to support cometabolic transformations by SRCs that produce alcohols is therefore strongly supported by prior physiological studies with diverse bacteria.

The main objectives of the study were to develop a method to co-encapsulate strain ATCC 21198 and TBOS or T_2BOS in GG hydrogel beads, and to evaluate the performance for achieving long-term cometabolic transformations in aerobic batch reactor systems. Specific objectives were to: 1) optimize the

co-encapsulation methods to produce mechanically stable GG macro-beads that maintained the microbial activity of strain ATCC 21198 and contained up to 10 % wt/wt TBOS and T_2BOS; 2) measure the abiotic rate of hydrolysis of TBOS and T_2BOS in aqueous suspension and in the co-encapsulated hydrogel GG macro-beads; 3) evaluate the ability of co-encapsulated strain ATCC 21198 to utilize 1-butanol and 2-butanol released from SRCs over an extended time period (300 days); 4) determine the cometabolic transformation rates of mixtures of 1,1,1-TCA, *cis*-DCE, and 1,4-D by the co-encapsulated cells with successive additions over time, and determine how the rates changed over time; 5) and assess the performance of the GG macro beads in groundwater/sediment microcosms from a contaminated site.

2. Materials and methods

2.1 Materials

All CAHs were purchased from Tokyo Chemical Industry (>98% purity), 1,4-D was purchased from J.T. Baker (>99%), and TBOS and T_2BOS were purchased from Gelest Inc. (>95%). 1- and 2-butanol used for calibration standards were purchased from Sigma-Aldrich (>99%). Isobutane was used for initial batch growth of strain ATCC 21198 culture and purchased from Gas Innovations (>99.99%). Sodium alginate was purchased from Spectrum Chemical and Gellan Gum (Kelcogel) was donated by C.P. Kelco. All other chemicals used in the study were of reagent grade.

2.2 Growth of 21198 for encapsulation and suspended cell tests

Rhodococcus rhodochrous ATCC 21198 was obtained from Dr. Michael Hyman, North Carolina State University and is commercially available from the American Type Culture Collection (ATCC). Details of the culture maintenance and batch growth are provided by Rolston *et al*. (2019)[19]. Strain ATCC 21198 was grown on isobutane in 720-mL glass bottles containing 270 mL of phosphate-buffered mineral salts medium (MSM) [44] and 450 mL of air headspace with 45 mL of isobutane added. The culture was incubated at 30°C on a rotary shaker table at 200 rpm and harvested by centrifugation when in late exponential growth phase. The cell pellet was resuspended in phosphate buffer (50 mM, pH 7.0) and centrifuged again. The washing was repeated, and the resting cell pellet was finally resuspended in buffer. The biomass concentration was determined using Total Suspended Solids (TSS) analysis as described in AWWA standards.[45] Under the growth conditions described above the ratio of protein to TSS was 0.45 mg protein/mg TSS.[19]

2.3 Encapsulation and Co-encapsulation

Strain ATCC 21198 was encapsulated separately in alginate and GG to enable comparisons between the two encapsulation methods and media. Details of the method used to encapsulate strain ATCC 21198 in alginate are provided by Rasmussen (2018)[46] and the Supplementary Information (SI). The GG

encapsulation method is more involved than alginate because gelation is a function of temperature as well as the crosslinking concentration.[34,35] The gelation process requires heating of pre-gel solution to at least 60°C followed by a direct addition of crosslinking cation salts or solutions, and cooling to below 45°C to initiate gelation. The temperature-dependent crosslinking of GG allows for the development of more simple emulsification internal gelation procedures.[47,48] The gelation method has been used to create highly stable spherical micro-beads ranging from below 20 µm to above 150 µm in size.[47] Methods developed here to co-encapsulate strain ATCC 21198 with the SRCs resulted in the production of macro-beads (~ 2 mm in diameter) that could potentially be used to create a permeable reactive barrier.

2.3.1 Encapsulation of strain ATCC 21198 in gellan-gum macrobeads

The following procedure was used to encapsulate strain ATCC 21198 in GG macrobeads that maintained high rates of microbial activity. The method developed follows a similar procedure presented by Hamid et al. (2014) and Li et al. (1996).[49,50] in which cylindrical macrobeads are created. A 0.75% (w/v) GG pre-gel solution was prepared in autoclaved phosphate buffer (~2mM, pH-7) at ~85°C. GG powder was added immediately after removing the solution from the autoclave. The pre-gel solution was shaken vigorously for 30 seconds and placed on a heated magnetic stir plate keeping the solution at ~85°C while mixing at 200 rpm for 30 minutes. A $CaCl_2$ solution was added to the pre-gel solution to achieve a final concentration of 0.06% (w/v) $CaCl_2$. The solution was allowed to cool to ~60°C and the pH was adjusted to 7 with dilute NaOH. The solution was then cooled to ~45°C and a known mass of strain ATCC 21198 from a concentrated slurry was added. Strain ATCC 21998 that was added was grown on isobutane and harvested at late exponential growth phase, as described above. At this stage the pre-gel solution was ready for gelation. The pre-gel solution was drawn into a 1.5m section of flexible rubber tubing with an inner diameter of ~2mm using an attached 60-ml plastic syringe (Figures S3-S5). The pre-gel solution was cooled to ~15°C, by setting the tubing on ice solidifying the gel within the tubing. The gel-filled tubing was then placed in a laminar flow hood for 60 minutes to provide extra time for internal crosslinking prior to extrusion of the gel. In a laminar flow hood, the solidified GG was pushed from the tubing onto long sections of Parafilm using an attached 60 mL syringe filled with air. The extruded sections of hardened GG were ~2 mm in diameter by ~15-30 cm in length. A sterilized razor blade was used to cut the long sections into ~2 mm sections, such that the height of each cylinder was approximately the same as the diameter. The cylinders were allowed to cure for an additional 10 minutes. The cylinder beads were then crosslinked by transferring them to a 1L beaker containing 500 mL of 0.25% (w/v) $CaCl_2$ solution and allowed to react for 60 minutes. The macro-beads were separated from the external crosslinking solution using a vacuum pump fitted with a 70 mm plastic filter funnel. The filtered beads were washed three times with carbonate buffered MSM (pH 7) and damp dried using the vacuum pump filter funnel. To calculate the final mass

loading of cells in beads (mg TSS/g bead), the assumption was made that 1 mL of pre-gel solution formed 1g of beads and that all cells added were encapsulated. Typically, microbially active beads were used for experimentation the day they were made; however, on occasion beads were stored overnight in pH 7 carbonate buffered MSM at 4°C.

2.3.2 Co-encapsulation of TBOS or T_2BOS and strain ATCC 21198 in gellan gum

The encapsulation of TBOS or T_2BOS in GG macrobeads required an additional step to the microbial encapsulation method presented above. That step required the emulsification of SRCs within autoclaved GG pre-gel solution prior to adding $CaCl_2$ crosslinking solution. After complete hydration of GG powder (as described above), a known volume of warm pre-gel solution, typically 40-50 mL, was transferred to an autoclaved-125 mL wide mouth glass vial. Span-80 emulsifier was added to achieve a concentration of 0.1% (v/v). A known volume of TBOS or T_2BOS was then added to the pre-gel solution and the mixture was emulsified using an IKA RW 20 digital overhead impeller mixer at 2500 rpm for 10 minutes. Following emulsification, the pre-gel solution was heated back to ~80°C and transferred to a 50 mL Falcon tube. To initiate gelation, an appropriate volume of 10% $CaCl_2$ stock solution was added to make a final concentration of 0.06% w/v. The solution was vortexed for 30 seconds. The pre-gel solution was then left at room temperature to cool to ~60°C before the pH was adjusted to 7 with dilute NaOH, if necessary. If co-encapsulation of cells was desired, the pre-gel solution was again left at room temperature to cool to ~45°C before adding cells. To create macro-beads from the warm pre-gel solution the tubing cooling and extrusion method described above was used. Microbially active macrobeads were separated from the external crosslinking solution using a vacuum pump fitted with a 70mm plastic filter funnel. To rinse any exogenous SRCs from the surface of beads, they were washed three times with a sterile and microbially safe 0.1% (v/v) Tween-80 soap. Finally, the beads were rinsed three times with carbonate buffered MSM (pH 7) and dried a final time using the vacuum pump.

In order determine the SRC mass loading in beads as g_{SRC}/g_{bead} and encapsulation efficiency of this process, 0.25 g samples of beads were transferred into 27 mL vials containing 10 mL of 2 mM sodium citrate solution. Sodium citrate was used to chelate calcium and help break apart the GG cylinders such that any encapsulated TBOS or T_2BOS was released into solution.[31,35] These vials were heated to ~80°C then placed on a shaker table shaking at 250 rpm for 120 minutes. The amount of encapsulated TBOS or T_2BOS was quantified using dichloromethane (DCM) extraction, and the known initial mass of beads broken down was used to determine a mass loading (g_{SRC}/g_{bead}). The amount of TBOS or T_2BOS in the extracted DCM was determined by GC analysis, as described in the analytical methods. The encapsulation process efficiency—the percent of added SRC that was successfully encapsulated—was then determined for the measured mass loading (g_{SRC}/g_{bead}), the measured final mass of beads (g_{bead}) and the known mass of added SRC.

2.4 Assessment of microbial activity after encapsulation

Short-term isobutane utilization tests were used to determine the immediate effect encapsulation had on cell viability. Batch reactor tests were conducted at 20°C in 27 mL crimp topped glass vials sealed with gray butyl rubber septa. Ten mL of carbonate buffered MSM (pH 7) was added to each sterile vial, followed by an addition of a known mass of suspended, encapsulated, or co-encapsulated bacterial cells ranging from 0.5-5mg cells as TSS. Isobutane (~8 µmol) was added to the vial headspace using a gas tight syringe. Vials were shaken rapidly on a rotary shaker table at 200 rpm to ensure equilibration of the headspace with the aqueous phase. Gas concentrations were determined by GC analyses of the headspace and were used to estimate the total dissolved mass using Henry's Law. Substrate utilization rates were calculated through linear regression of isobutane mass data *versus* time and the cell mass added to each reactor. Suspended cell substrate utilization rates were used as a benchmark to assess the effect encapsulation had on cellular viability.

2.5 Long-term cometabolic transformation experiments

Batch reactors were used to evaluate the long-term transformation performance of co-encapsulated strain ATCC 21198 with TBOS or T_2BOS. These tests were conducted in 125 mL and 250 mL glass Wheaton serum bottles with nominal volumes of 155 or 310 mL, respectively. The serum bottles (batch reactors) were sealed with screw on caps fitted with gray butyl rubber septa. The serum bottles were filled with 100 or 200 mL of carbonate-buffered MSM (pH 7) followed by an addition of suspended, encapsulated, or co-encapsulated cells to achieve an initial cell concentration of 10 mg-TSS/L. Encapsulated bead cell mass loadings as g_{TSS}/g_{bead} were used to determine the mass of beads to add to each reactor. With initial encapsulated cell mass loadings of 0.5 mg_{TSS}/g_{bead}, 2 g of beads were added to the serum bottles for co-encapsulated treatments and 1 mg of cells to the suspended treatments so the cell concentrations were ~10 mg/L.

Due to mixtures being frequently observed at contaminated sites, the ability of strain ATCC 21198 to transform a mixture of 1,1,1-TCA, *cis*-DCE, and 1,4-D was evaluated. The reactors received initial and/or successive additions of environmentally-relevant aqueous concentrations of each contaminant (~250-1000 µg/L). CAHs were introduced via additions of Nanopure water saturated with the CAH of interest and 1,4-D was added from a 1000 ppm stock solution. Controls without cells or beads were used to monitor abiotic losses from the reactors. To monitor the potential mass of alcohol being released from encapsulated SRCs, several reactors with co-encapsulated cells were poisoned with 2% (w/v) sodium azide to ensure cells would not consume the hydrolysis byproducts. These reactors were used to determine the rates of abiotic

hydrolysis described below. Reactors were monitored over a period of 0 to 303 days for respiration data (headspace concentrations of O_2 and CO_2), alcohol and 1,4-D concentrations in the bulk aqueous phase, and headspace concentrations of 1,1,1-TCA and *cis*-DCE using analytical methods described below. The batch reactors were incubated at 20˚C on a shaker table at 100 rpm. The shake speed was reduced from 200 rpm to 100 rpm to lessen the abrasion of the beads, however the long incubation time ensured Henry's Law equilibrium was maintained. The continuous shaking also helped to determine the long-term mechanical stability of the GG beads.

2.6. Microcosm experiments with groundwater and aquifer sediments and GG beads

Microcosm reactors were constructed using the same procedures as described in section 2.5, but media was replaced with groundwater and aquifer solids from a site contaminated with 1,4-D and a mixture of CAHs. Procedures for the microcosm construction are provided by Rolston et al. (2019)[19]. The microcosms were constructed in sterile, 125 mL glass Wheaton serum bottles sealed with reuseable screw caps fitted with gray butyl rubber septa. Each microcosm contained 15 mL of mixed core material obtained from three depths from the aquifer and 50 mL of site groundwater. Prior to the addition of the GG beads the microcosms were purged with N_2 gas for several hours to remove volatile site contaminants, which permitted the same contaminant mixture of 1,1,1-TCA, *cis*-DCE, and 1,4-D as tests in media (section 2.5) to be assessed. Beads co-encapsulated with strain ATCC 21198 and TBOS were then added at the same SRC mass loading and cell mass loading (2 gm of beads at 0.5 mg_{TSS}/g_{bead}) to the buffered media batch reactors permitting a direct comparison between the two treatments. Acetylene controls (a known SCAM inhibitor) were constructed by adding 1.0 mL of acetylene to a batch reactor headspace. Repeated additions of a mixture of 1,1,1-TCA, *cis*-DCE and 1,4-D were added as described above.

2.7 Abiotic hydrolysis experiments

The rates of hydrolysis of TBOS and T2BOS were determined using methods previously described by Varcheeswaran *et al*. (1999)[40]. Batch reactors that were poisoned, as described above, were used to determine the rate of hydrolysis both in suspension and released from GG co-encapsulated beads at different mass loadings in GG. These batch kinetic tests were conducted in 125 mL glass Wheaton serum bottles sealed with reusable screw caps fitted with gray butyl rubber septa. Reactors were filled with 100 mL of carbonate-buffered MSM (pH 7), followed by an addition of free suspended or encapsulated SRCs. The total mass of TBOS or T_2BOS added to each reactor ranged from 1000-1500 mg/L. O_2 and CO_2 concentrations were monitored to demonstrate no microbial activity occurred in the poisoned controls and served as an additional control. The batch reactors were incubated at 20˚C on a shaker table at 100 rpm.

2.8. Analytical methods

All volatile compounds (O_2, CO_2, isobutane, *cis*-DCE, 1,1,1-TCA, 1,1-DCE, and VC) were measured by sampling the gas headspace with 100 µL gas tight Hamilton syringes followed by injection

into a Hewlett Packard (HP) 5890 or 6890 series gas chromatograph (GC). Isobutane was measured using HP 6890 series GC equipped with a flame ionization detector (FID). Isobutane was separated using an Agilent GS-Q capillary column (30m x 0.53mm) with He as the carrier gas (15 mL/min) at 150°C, resulting in a retention time (RT) of 0.8 min. A HP 6890 series GC equipped with a micro-electron capture detector (ECD) was used to measure 1,1,1-TCA and *cis*-DCE. 1,1,1-TCA and *cis*-DCE which were separated with an Agilent DB-624 UI capillary column (30m x 0.53mm) with He as the carrier gas (15 mL/min) at 50°C resulting in *cis*-DCE and 1,1,1-TCA RT of 2.0 and 2.4 min, respectively. O_2 and CO_2 were measured using HP 5890 series GC equipped with thermal conductivity detectors (TCD). O_2 and CO_2 were separated using a Supelco 60/80 Carboxen-1000 packed stainless-steel column (15ft x 1/8in.). The O_2 method used He as the carrier gas (30 mL/min) at 40 °C, while CO_2 used argon as the carrier gas (30 ml/min) at 220 °C. The GC methods were calibrated using external standards.

The total masses in the reactors were determined using the measured headspace concentrations and by applying Henry's Law.

$$Total\ Mass = C_g * V_g + \frac{C_g}{H_{cc}} * V_L \qquad (1)$$

Where:

$C_g =$ *Headspace Gas Concentration,* $H_{cc} =$ *Henry's Law Constant*

$V_g =$ *Volume of Headspace,* $V_L =$ *Volume of Liquid*

1- and 2-butanol produced from the hydrolysis of TBOS and T_2BOS respectively, were measured using a HP 5890 series GC equipped with an FID. A 5µL liquid sample was injected onto a Supelco 80/100 Carbopack-C packed column (6 ft x 1/8 in) with N_2 as the carrier gas and chromatographic separation was achieved at 105°C.

1,4-D was analyzed from aqueous samples using a Hewlett Packard Series 6890 Gas Chromatograph-Model 5973 Mass Spectrometer (GC-MS) preceded by a Tekmar Dohrmann Model 3100 heated purge and trap concentrator. Details of the analytical method are described by Rolston et al. (2019)[19]. The GC-MS was run in single ion mode for m/z 88 (1,4-D) and m/z 96 (deuterated 1,4-D run as an internal standard.[51] The 1,4-D quantification limit was 1 x 10^{-4} mg/L, however 25-ml was required for each 1,4-D sample. Due to the large volume and the sensitivity of the instrument, most samples from the batch reactors were diluted 125 to 250 times.

The mass of TBOS and T_2BOS encapsulated in GG beads was determined in the liquid produced from GG beads after treatment with sodium citrate by liquid-liquid (dichloromethane-aqueous) extractions,

as described by Vancheeswaran et al. (1999).[40] The reactors were vigorously shaken for 30-60 seconds to ensure adequate homogenization of TBOS and T_2BOS and surrounding media. The sampled liquid (1 ml) was directly added to 1 mL DCM containing 3000 mg/L tetra-*n*-propoxysilane (TPOS) as an internal standard. These samples were then vortexed for 15 min in 4 mL gas tight glass vials.

The liquid DCM was separated from the aqueous sample and transferred into 2 mL gas tight glass auto-sampler vials with rubber septa. Vials were loaded onto a Hewlett Packard HP 6890 Series auto-sampler that automatically injected 5 µL DCM liquid samples onto the GC. The GC was equipped with a Restek RTX-20 capillary column (15m x 0.53 µm) and an FID detector. Helium was the carrier (12 mL/min) with an initial oven temperature of 100°C. The initial temperature was held for one minute followed by a 35°C/minute temperature ramp to 220°C, which was held to a final run time of 5 minute. DCM, TPOS, T_2BOS, and TBOS peaks had RTs of 0.8, 3.2, 3.9, and 4.3 minutes, respectively. Concentration measurements were converted to total mass in the beads.

3. Results

3.1. Cell viability after encapsulation

Cell viability experiments were performed after optimization of encapsulation methods to determine the activity of strain ATCC 21198 in both alginate and GG matrices. The utilization rates of isobutane in the beads were compared with those of suspended cells (Figure 1 and Table S1). Alginate macrobeads were spherical and ~2 mm in diameter (Figure S2) while GG macrobeads were cylindrical and ~2 mm in diameter by ~2 mm tall (Figure S6). The results show very similar isobutane utilization rates for encapsulated cells compared to suspended cells. Zero-order rates achieved in encapsulated cells were approximately 90% of those obtained by cells in suspension. Encapsulated cells often experience rate limitations in comparison to suspended cells due to slow O_2 or substrate diffusion into hydrogel beads.[52,53] One explanation for the observed similarity in isobutane-utilization rates between encapsulated and suspended cells is the relatively low mass loading of cells within the beads (~0.5 mg_{TSS}/g_{bead}). In most hydrogel diffusion and utilization studies the cell mass loading are greater than 10 mg_{TSS}/g_{bead}.[53] Hiemstra *et al*. (1983)[53] investigated the influence of cell mass loadings in alginate macro-beads and found that the higher the mass loading of cells the greater diffusion inhibited O_2 utilization. Overall, the isobutane utilization rate tests demonstrated that strain ATCC 21198 could successfully be encapsulated in both alginate and GG hydrogels with minimal to no loss in metabolic activity.

3.2 Rates of abiotic hydrolysis of TBOS and T_2BOS encapsulated in alginate and GG beads

The rates of abiotic hydrolysis of TBOS and T_2BOS encapsulated in alginate and GG beads was determined in batch reactor tests. Previous research indicated that the non-aqueous phase concentration of

TBOS in solution affected the rate of hydrolysis.[40] The mass loading of TBOS and T_2BOS in the aqueous phase of the batch reactors were therefore kept the same for the suspended and GG bead tests. The concentrations of TBOS and T_2BOS in abiotic poisoned reactors were the same as in the live biotic reactors containing GG beads (1000-1500 mg/L) and had the potential to produce 1300-1920 µmols of the alcohols

The initial abiotic hydrolysis tests were conducted with TBOS encapsulated in alginate macrobeads at a mass loading of 5 and 30% (wt/wt). The beads were added to 100 ml of carbonate- buffered media (pH 7), to achieve an initial TBOS concentration of 1000 mg/L; 2 grams of 5% beads and 0.33 grams of 30% beads were added. The reactors were shaken at 100 rpm on a rotary shaker table to provide good mixing, while avoiding abrasion of the beads. The reactors were monitored for 1-butanol production over 140 days (Figure 2 Top) and the zero-order production rates were determined via linear regression (Table 1). The hydrolysis reaction was well fit by a zero-order rate estimate for both suspended and encapsulated results. The rate of 1-butanol production was an order of magnitude greater when TBOS was in free suspension than when encapsulated (Table 1). One possible explanation for the higher hydrolysis rate of TBOS in suspension is that an emulsion formed in the aqueous phase while shaking the reactors at 100 rpm. This provided a large surface area for hydrolysis and mass transfer to occur. In the reactors containing alginate beads TBOS droplets are dispersed within the hydrogel and the hydrolysis reaction was likely mass transfer limited. The results also showed that when TBOS was encapsulated in alginate at ~30% (w/w) it hydrolyzed at half the rate of TBOS encapsulated in alginate at ~5% (w/w). However, the mass of beads present was 6 times lower for the 30% case. Based on the measured zero-order rate of hydrolysis and the assumption that the rate remained constant with time, the beads were estimated to produce 1-butanol for 5 and 10 years at loading rates of 5 and 30% at the mass loading of the reactors.

Table 1. Abiotic rates of hydrolysis of TBOS in alginate macrobeads and suspended in solution with estimated lifetimes of encapsulated TBOS.

Treatment	Added Initial TBOS Mass (µmol)	Maximum Possible Butanol Release (µmol)	Butanol Production Rate (µmol/day)	Estimated Exhaustion of TBOS (years)
Suspended TBOS	312	1250	5.9	0.6
Encapsulated TBOS (5% w/w)	326	1310	0.69	5.2
Encapsulated TBOS (30% w/w)	324	1300	0.35	10.1

The rates of abiotic hydrolysis of TBOS and T_2BOS encapsulated in GG beds was also determined. Both SRCs were encapsulated in cylindrical GG macro-beads (Figure S6) at mass loadings of ~8% (w/w).

Cells of strain ATCC 21198 were also co-encapsulated within the GG hydrogel at initial concentrations of ~0.5mg_{TSS}/g_{bead} with sodium azide (0.2% (w/v) added as a cellular poison. Two grams of beads were added to each abiotic reactor such that a final concentration of ~1500 mg/L TBOS and T_2BOS was achieved. Reactors containing suspended T_2BOS at ~1500 mg/L were created for comparison.

Table 2. Abiotic rates of hydrolysis of T_2BOS and TBOS in gellan gum macrobeads and suspended in solution with estimated lifetimes of encapsulated T_2BOS and TBOS.

Treatment	Added Initial TBOS Mass (µmol)	Maximum Possible Butanol Release (µmol)	Butanol Production Rate (µmol/day)	Estimated Exhaustion of TBOS (years)
Suspended T_2BOS	475	1900	0.20	26
GG Encapsulated T_2BOS (8% w/w)	441	1770	0.050	97
GG Encapsulated TBOS (8% w/w)	479	1920	1.3	4.0

The results of the hydrolysis rate tests with T_2BOS are presented in Figure 3. Some 2-butanol was present in the T_2BOS (95% purity) that was used for encapsulation resulting in 2-butanol being initially present. Zero-order rates of hydrolysis fit the results fairly well, as indicated by the linear regressions. The GG encapsulated T_2BOS hydrolyzed a factor of four slower than the suspended T_2BOS (Figure 3, Table 2), which is consistent with observations of TBOS encapsulated in alginate (Table 1). GG-encapsulated TBOS hydrolyzed ~2 times faster than alginate-encapsulated TBOS (Figure 2). The greater mass loading in GG of 8% wt/wt compared to 5% wt/wt in alginate may be partly responsible for the higher rates. Both encapsulation in alginate and GG resulted in factors of 4 to 10 lower rates of hydrolysis than observed in solution at the same mass loadings. The rate of hydrolysis of TBOS encapsulated in GG was 27 times greater T_2BOS, at mass loadings of ~8% (wt/wt) (Table 2), while in solution TBOS hydrolyzes ~30 times more quickly than T_2BOS. This is consistent with previous research where the more sterically hindered the central silicate is by the leaving groups, the less access water has to hydrolysis sites.[38,39] The slow rate of hydrolysis of T_2BOS in GG would potentially provide for a very long life of the substrate to promote aerobic cometabolism.

3.3 Long-term cometabolic transformation studies with GG beads co-encapsulated with strain ATCC 21198 and SRCs

Batch reactor experiments were conducted to determine if strain ATCC 21198 could maintain long-term cometabolic treatment of a mixture of 1,1,1-TCA, *cis*-DCE, and 1,4-D when co-encapsulated with

TBOS or T_2BOS. The experiments were conducted with cylindrical GG macro-beads containing strain ATCC 21198 and TBOS or T_2BOS with biomass loadings of ~0.5mg_{TSS}/g_{bead} and SRC mass loadings of ~8% (w/w) SRC. Two grams of beads were added to the batch reactors, to achieve final cell concentrations of ~10 mg_{TSS}/L and SRC concentrations of ~1500 mg/L. A control with no addition of beads was used to monitor for abiotic losses. Suspended cell controls with the same biomass as encapsulated in the GG beads, but with no SRC added illustrated the effect of co-encapsulation on initial and long-term cell viability. Reactors were created in duplicate or triplicate.

3.3.1 Respiration activity of ATCC 21198 co-encapsulated with TBOS

Figure 4 presents respiration (O_2 and CO_2), cometabolic transformation (1,1,1-TCA, *cis*-DCE, and 1,4-D), and substrate (1-butanol) results for the batch reactors with GG beads that contained cells of strain ATCC 21198 co-Encapsulated with TBOS (CET), along with the abiotic control data. There was a lag in O_2 utilization and CO_2 production, with O_2 depleted during the first 30 days of incubation. After O_2 was depleted due to cellular respiration, pure O_2 was added to the reactor headspace. The results from the abiotic control and the suspended cell reactors (Figure S7) show little uptake of O_2 or change in the CO_2 concentration. The repetitive decrease in O_2 concentrations and constant increase in CO_2 within CET reactors, in comparison to suspended cell control reactors, demonstrates cellular respiration was occurring in the CET reactors. (Figure 4 A-B).

The O_2 utilization in the CET reactors increased by 3-4 times from the initial observed rate to the rate observed after the second addition of O_2. However, after a subsequent third and fourth addition of O_2, the O_2 uptake rate remained fairly constant (Table S2). The observed increase in O_2 consumption rates indicates that microbial growth likely occurred within CET reactors with a plateauing of rates in subsequent additions over 60 days of incubation. The O_2 consumption results support a pseudo-steady-state biomass concentration being reached in the beads. The continuous increase in headspace CO_2 concentrations supports the O_2 utilization results. Results from the suspended cell control reactors are shown in Figure S7. Minimal O_2 utilization or CO_2 production was observed in the suspended cell controls.

The observed O_2 utilization and CO_2 production in CET reactors is due to cellular utilization of 1-butanol released from the hydrolysis of encapsulated TBOS. An elevated O_2 consumption rate was estimated for CET-B reactor compared to CET-A reactor (Table S2). It is not known why the duplicates behaved differently, but this would be expected in long-term incubations during which both microbial growth and decay occurs. The utilization of 1-butanol that resulted from TBOS hydrolysis is also supported by measurements of 1-butanol concentration in the bulk solution of active CET reactors compared to the poisoned control (Figure 4F). The 1-butanol concentrations in the bulk solution of the CET reactors were typically below the detection limit (~1 mg/L), while the continuous increase in 1-butanol was observed in

the poisoned controls. The results support the utilization of 1-butanol produced by TBOS hydrolysis by strain ATCC 21198 co-encapsulated in the GG beads (Figure 4F).

Another line of evidence confirming that the production of 1-butanol from encapsulated TBOS is driving O_2 utilization and CO_2 production within CET reactors, is the comparison of O_2 and 1-butanol results around 30 days of incubation, when reactor CET-B went anoxic. Due to a vacuum that develops in the reactors, and the method of sampling used (that permits air to enter sampling syringe after it is withdrawn from the reactor), a reported O_2 mass of ~180 µmol represents anoxic conditions in the reactors. When the reactor went anoxic, 1-butanol was detected in the bulk solution (Figure 4F). After O_2 was added to the CET-B reactor headspace, the 1-butanol decreased back below the detection limit, providing evidence that O_2 utilization within these reactors is due to cellular oxidation of 1-butanol released from encapsulated TBOS. This period of going anoxic may partly be responsible for the deviation in performance of the duplicate reactors.

Stoichiometric analysis also indicates O_2 consumption and CO_2 production were due to cellular utilization of 1-butanol released from TBOS. The amount O_2 utilized within CET reactors over the first 70 days of incubation was 930 and 1320 µmol in the CET-A and CET-B reactors, respectively. The amount of 1-butanol released via abiotic hydrolysis in the poisoned control over 70 days, estimated from the abiotic hydrolysis rate of 1.3 µmol/day, (Table 2) is 91 µmol. Based on 6 µmol of O_2 required to oxidize 1 µmol of butanol to CO_2 and H_2O (assuming no cell yield), 550 µmol of O_2 would be required. CO_2 mass balances were also performed using the reactor headspace CO_2 concentrations and Visual Minteq (2005)[54] calculations, and assuming a buffered pH of 7.0 to determine the aqueous mass of H_2CO_3 and HCO_3^- [i].The estimated mass of CO_2 produced is 550 µmol which is in good agreement with the amount expected to be formed, assuming no cell yield. The amount of O_2 consumed in the biotic reactors was about twice that predicted based on 1-butanol released by abiotic hydrolysis in the poisoned control. However, this estimate does not consider butanol utilized for cell yield and maintenance, which would decrease the amount of 1-butanol respired to CO_2 and H_2O. The O_2 required to oxidize the three contaminants (1,1,1-TCA, *cis*-DCE, and 1,4-D), would also contribute to the O_2 demand. Assuming the contaminants were oxidized to CO_2, H_2O, and Cl^-, their transformation contributed to on average 0.45%, 0.29%, and 2.9% of the total O_2 consumed in the CET-A and CET-B, over the initial 70 days of incubation. The O_2 respiration results indicate that the rate of hydrolysis in the live reactors was greater than expected from the rates of abiotic hydrolysis to produce 1-butanol, while CO_2 production was close to that expected. Both estimates indicate that the production of 1-butanol from the abiotic hydrolysis is supporting the microbial metabolism.

3.3.2 Cometabolic transformation by ATCC 21198 in the CET reactors

Based on the respiration data in CET reactors, it is apparent that the biomass is active and TBOS hydrolysis is supporting the biomass of strain ATCC 21198 in the GG beads. The observed microbial activity translated into cometabolic transformation of 1,1,1-TCA, *cis*-DCE and 1,4-D (Figure 4 C-E). The CET reactors received and transformed five additions of the contaminant mixture, three at the initial mass amount and two at approximately double the initial mass amount. In contrast, suspended cell control reactors that contained a similar initial biomass received multiple additions of contaminants (Figure S7) but only transformed the first addition. Limited resting cell transformation was achieved by the suspended biomass that had been grown on isobutane. A long-term slow decrease of *cis*-DCE was also observed that may have been cometabolic in nature. Continuous transformation of 1,1,1-TCA, *cis*-DCE and 1,4-D was observed in the CET reactors. *Cis*-DCE was transformed most rapidly, while 1,1,1-TCA and 1,4-D were transformed at similar first-order rates. The rates of transformation of 1,1,1-TCA, *cis*-DCE, and 1,4-D within CET reactors achieved in the four additions were similar over the duration of the experiment (Figure 4 C-E). In the reactors with suspended cells, but with no substrate added (Figure S7), the three contaminants were initially transformed, but the transformation ceased after the first addition. Of note is the lag in transformation of the contaminants observed in reactor CET-B, just after the third contaminant addition at 30 days when the reactor went anoxic. The absence of O_2 is consistent with the observed lack of transformation of 1,1,1-TCA and *cis*-DCE. After the addition of O_2 at ~45 days, cometabolic transformation of contaminants proceeds at rates similar to reactor CET-A.

The observations support continuous cometabolic transformation activity associated with the microbial activity in the GG beads. Strain ATCC 21198 utilizes the 1-butanol released from encapsulated TBOS and uses oxygenase enzymes that are expressed under these conditions to enable cometabolic transformations. The data collected in CET reactors indicate that 1-butanol bulk aqueous concentrations are kept low by the combined effects of microbial activity and the slow hydrolysis of TBOS. The long-term transformation of the final addition will be discussed in a subsequent section.

3.3.3 Respiration activity of strain ATCC 21198 co-encapsulated with T_2BOS

Batch reactor tests were conducted with cells of strain ATCC 21198 co-encapsulated with T_2BOS in GG (CET_2) that replicated the tests with TBOS discussed above. Figure 5 presents respiration (O_2 and CO_2), cometabolic transformation (1,1,1-TCA, *cis*-DCE and 1,4-D), and substrate data (2-butanol) collected for CET_2 reactors (A, B, and C) that contained the GG beads co-encapsulated with T_2BOS and strain ATCC 21198. O_2 and CO_2 results for the CET_2 reactors show much lower cellular activity compared to CET reactors with encapsulated TBOS. Minor decreases in O_2 concentration were observed in relation

to suspended cells (Figure S7) or abiotic reactors over the initial ~70 day period (Figure 5 A-B). However, linear regression of the O_2 mass of time-series, shows significant differences relative to suspended and abiotic controls. O_2 within the CET_2 reactors headspace decreased at a significant zero-order rate compared to the controls (Table S3). The much lower rate of O_2 consumption in CET_2 reactors compared to CET reactors is consistent with the much lower abiotic hydrolysis rate of T_2BOS compared to TBOS (Table 2). The rate of O_2 utilization of 0.48 µmol/day (Table S3) in the CET_2 reactors, compared with 18 to 40 µmol/day for the CET reactors. The factor of 40 to 80 times higher rate O_2 utilization rate in the CET reactors is consistent with the 27 times higher rate of alcohol production when TBOS was encapsulated in GG beads compared to T_2BOS (Table 2).

Based on the estimated abiotic hydrolysis rate of the encapsulated T_2BOS of 0.05 µmol/day, (Table 2) after 70 days approximately 3.5 µmol of 2-butanol would be produced (Figure 5F). This would require ~21 µmol of O_2 to oxidize it to CO_2 and H_2O (assuming no cell yield). Based on a measured O_2 utilization rate of 0.48 µmol/day, ~34 µmols of oxygen were consumed in CET_2 reactors after 70 days of incubation. These results are consistent with observations with encapsulated TBOS, that observed O_2 utilization rates were about twice those estimated from the rates of hydrolysis, which might result from biotic hydrolysis of T_2BOS. The estimates support the observed utilization of O_2 due to microbial consumption of 2-butanol being slowly hydrolyzed from encapsulated T_2BOS. The analysis indicates that respiration due to cellular activity is occurring within CET_2 reactors when compared to suspended cell controls, with considerably slower activity in comparison to the CET reactors, which is consistent with the much slower rates of hydrolysis. Figure 5F shows some detection of 2-butanol in the bulk solution, but concentrations tend to be below 1 mg/L. Thus, the encapsulated cells are effective in utilizing the 2-butanol produced via hydrolysis.

3.3.4 Cometabolic transformations by strain ATCC 21198 in the CET_2 reactors

Respiration data for the CET_2 batch reactors indicate that there is much lower cellular activity occurring compared to the CET reactors. However, three consecutive additions of the 1,1,1-TCA, *cis*-DCE, and 1,4-D mixture were transformed in CET_2 reactors, all at concentrations similar to the CET reactors. CET_2 reactors transformed the majority of contaminants after 80 days of incubation, with *cis*-DCE most rapidly transformed and 1,1,1-TCA and 1,4-D more slowly transformed (Figure 5 C-E). In contrast to suspended cells stalling in transformation after the first addition when compared to the abiotic control (Figure S7), CET_2 reactors continued to transform all three contaminants at appreciable rates. This data indicates that in CET_2 reactors, the slow hydrolysis of T_2BOS and resulting consumption of 2-butanol produced, maintained microbial activity and cometabolic transformation of 1,1,1-TCA, *cis*-DCE, and 1,4-D. While the rates were slower than those observed in the CET reactors, the rate of O_2 consumption was

much lower. The low O_2 demand observed in CET_2 reactors, in comparison to the mass of contaminants transformed, is a very positive result, since O_2 will likely be a limiting factor in contaminated aquifers.

3.3.5 Long-term cometabolic transformations in the CET and CET_2 Reactors

Figure 4 presents the continued monitoring of the CET reactors for an incubation period of 300 days. O_2 continues to be depleted due to cellular respiration, and in the headspace O_2 was added numerous times to ensure that aerobic respiration and cometabolism proceeded. The repetitive decrease in O_2 and constant increase in CO_2 within CET reactors is apparent. The rate of O_2 utilization decreased in the last two additions on days 150 and 180, consistent with the decreased rate of CO_2 production. Very consistent trends in both O_2 consumption and CO_2 production were observed in the duplicate reactors. O_2 consumption rates decreased by about a factor of two, from an estimated rate of 11.6 µmol/day over the period of 90 to 120 days to an estimated 5.3 µmol/day over the period of 180 to 260 days (Figure S9). This decrease is consistent with the decrease in rate of CO_2 accumulation in the reactors headspace. These O_2 consumption results combined with the continued CO_2 production indicate continuous microbial activity over the 300-day incubation period.

Continued cometabolic transformation of the last addition of 1,1,1-TCA, *cis*-DCE, and 1,4-D was observed in the duplicate CET reactors over the period of 90 to 300 days. First-order plots are presented in Figures S10 to S12 for an earlier time period and a later time period and are summarized in Figure 6. *Cis*-DCE was most rapidly transformed at a first-order rate about 10 times greater than 1,1,1-TCA, while 1,4-D was transformed at twice the rate of 1,1,1-TCA. All three contaminants were more rapidly transformed in one of the duplicate reactors, illustrating a consistent cometabolic processes. It is not known why the treatments deviated among the duplicates, since rates of O_2 utilization and CO_2 production of the duplicate reactors were similar over this period. The deviation occurred, however, after the CET-B went anoxic.

Transformation rates within CET reactors of 1,1,1-TCA, *cis*-DCE, and 1,4-D slowed with time (Figure 6). The decrease in these rates are consistent with the decreased rate of O_2 utilization and CO_2 production. The observations of maintained transformation abilities and continued cellular activity suggest that co-encapsulated microorganisms utilizing 1-butanol released from encapsulated TBOS are able to maintain cometabolic activity for over 300 days, however the rate of transformation slowed in the final addition.

Figure 5 presents the continued monitoring of the respiration data (O_2 and CO_2), cometabolic transformation data of 1,1,1-TCA, *cis*-DCE and 1,4-D, and substrate data (2-butanol) collected for live CET_2 reactors A, B, and C along with the abiotic control reactor data. CET_2 reactors continued to show very slow rates of O_2 consumption over the extended time period, and therefore, no additions of O_2 were

made to the reactor headspace. Continued O_2 utilization was observed in CET_2 reactors compared to the control over the period of 90 to 230 days (Figure S8). CO_2 production above the abiotic control was also observed. Both the O_2 uptake and the CO_2 production provide evidence of slow cellular activity over the 300-day incubation period (Figure 5 A-B) with continued O_2 utilization and CO_2 production compared to the control.

Four consecutive additions of the chosen contaminant mixture were transformed by CET_2 reactors, all at levels similar to CET reactors. CET_2 reactors transformed the majority of the contaminants added, with the exception of 1,1,1-TCA, which has the lowest transformation rate of the mixture (Figure 5 C-E). The log plot of concentration *versus* time for the CET_2 for the earlier and extended time periods are shown in Figure S13 to S15 and rates are summarized in Figure 6. The results show the transformations followed first-order kinetics fairly well.

The co-encapsulated cometabolic transformation potential was maintained for over 300 days at very slow rates of O_2 utilization (Figure S8). Acontinuous long-term cometabolic transformation is indicated by the first-order plots shown in Figures S13 to S15. First-order transformation continued over the period of 80 to 300 days. For example, 1,1,1-TCA shows first-order kinetics up to around 300 days. *Cis*-DCE, which was transformed at the highest rate, fit first-order kinetics very well with a reduction in concentration by two orders of magnitude achieved in both of the time periods that were plotted. The first-order rate coefficients showed consistent decreases in the last transformation compared to the previous (Figure 6, Figures S13-S15). The first-order rate coefficient decreased by factors of 2.5, 2.6, and 1.8 for 1,1,1-TCA, *cis*-DCE, and 1,4-D, respectively. The decreases in the rates support the slowing of the same cometabolic process. One likely explanation is that the biomass of strain ATCC 21198 that is being supported by the hydrolysis of T_2BOS decreased by about a factor of two. More work is needed to determine factors responsible for the decrease in rates.

It is interesting to note that the CET_2 reactors rates of transformation slowed to a lesser extent than the CET reactors, whose first-order rate coefficient decreased by factors of 6 to 7 (Figure 6). The results suggest that the higher biomass being supported by faster rates of TBOS hydrolysis were not being maintained as well as the lower biomass supported by T_2BOS. The fit of the first-order rates also generally were better for the CET_2 reactors compared to the CET reactors, with R^2 values ranging from 0.953 to 0.995 for the CET_2 reactors compared with 0.921 to 0.973 for the CET reactors. The CET reactors show some slowing in rates over the time period of the regression, which result in a poorer fit. An example is the *cis*-DCE in the CET reactor over the period of 75 to 160 days (Figure S11). A faster rate is shown early on with a slowing in the rate later, resulting in deviations for the first-order regression ($R^2 = 0.947$). Over the same time period in the CET_2 reactors (75 to 172 days) the first-order model fits the entirety of the *cis*-DCE time series very well ($R^2 = 0.994$) (Figure S15). The changes in rates of O_2 consumption with time support

a greater slowing in the CET reactors versus the CET_2 reactors. Regression plots of zero-order O_2 mass decreases with time in the reactors are shown in Figures S8 and S9. In the CET reactors, the rate of O_2 consumption decreases by a factor of 4 over the three regression periods. Over the latter period the O_2 consumption rate was 5.3 µmol/day. The rates for the CET_2 reactors for the linear regression over 40 to 70 days show no observable uptake, while from 70 to 300 days the utilization rate increased to 0.62 µmol/day, a factor of 9 lower than the CET reactors.

3.4 VC and 1,1-DCE transformation in the CET and CET_2 reactors

To examine the cometabolic activity in the reactors with other CAHs, VC and 1,1-DCE was added to the CET and CET_2 reactors, on days 264 and 286, respectively. VC was transformed below the detection limit within a week in the TBOS (CET) and T_2BOS (CET_2) reactors (Figure **7**A). The fastest rate was achieved in a reactor that contained twice as many beads (2X) as the CET_2 reactors. The reactor with 2X the amount of beads was constructed at the same time as the CET2 (1X) reactors and was subjected to similar multiple exposures of the contaminants. Similar rates were achieved in the CET and CET_2 reactors that had the same mass of beads. In batch, resting cell transformation experiments with isobutane-grown cells of strain ATCC 21198, VC was transformed at a very high rate (~19 µmol/mg_{TSS}/day), compared to *cis*-DCE that was transformed at 3 µmol/mg $_{TSS}$/day.[17] The high VC rate observed is consistent with the high rate observed with isobutane grown cells. 1,1-DCE transformation was slower than VC in both CET and CET_2 reactors, while the CET_2 reactor with twice the mass of beads, transformed 1,1-DCE at the highest rate, consistent with the VC test **(**Figure **7**B). The results demonstrate 1,1-DCE transformation capability after 287 days of bead incubation. It should be noted that 1,1,1-TCA continued to be transformed during the period of the VC and 1,1-DCE tests (Figure S13.).

3.5 1,4-D Transformation of 1,4-D to Low Concentrations in the CET and CET_2 Reactors

After the slowdown of transformation rates of 1,1,1-TCA, *cis*-DCE, and 1,4-D, the concentrations of 1,4-D were monitored to ppb levels using a heated purge-and-trap GC/MS method. Lower detection limits were achieved by adding a larger volume of aqueous sample to the purge-and-trap. Figure 8 (A-C) shows 1,4-D concentration data in the CET and CET_2 reactors from 70-303 days of incubation on a log-scale. The decrease in concentration tracked first-order kinetics fairly well. Figure 8 (lower left) shows the log plot of 1,4-D concentration versus time in the CET reactors with beads co-encapsulated with TBOS and strain ATCC 21198. The 1,4-D concentrations were reduced to 13.3 ppb, representing over a 2-order of magnitude decrease in concentration. Similar results were observed with the CET_2 reactors (Figure 8 – upper left), where the 1,4-D concentration was reduced to 5.5 ppb, though with a slightly higher first-order rate constant compared to the CET reactor. When the amount of beads containing T_2BOS was increased by

a factor of 2, 1,4-D transformation rate increased by a factor of 1.45 and the 1,4-D concentration was reduced to 0.5 ppb (Figure 8 -upper left). Overall cometabolic transformation of 1,4-D fit a first-order rate model and was able to reduce the 1,4-D concentration to 0.5 ppb, which may be required for in-situ treatment.

3.6 Incubation of GG beads co-encapsulated with TBOS and strain ATCC 21198 in microcosms with aquifer material and groundwater from a contaminated site

One potential use of the technology is to create a permeable reactive barrier by mixing the co-encapsulated beads with aquifer solids. A batch microcosm study was performed to test this concept. The microcosms were constructed with groundwater and aquifer material from a contaminated site as described in the methods section. GG beads that were co-encapsulated with TBOS and strain ATCC 211198 were synthesized as described in methods and added to the microcosms in the same mass amount (2 g) as used in the tests previously described. TBOS was chosen as the SRC to provide a more rapid response in the microcosms. These beads were made separately than those used to generate the results presented previously. However, in order to make a direct comparison with the batch tests performed previously in media, treatments with media only were made that replicated those used to generate results presented in Figure 4. The media treatment was constructed and operated at the same time as the microcosms.

These tests also evaluated the reproducibility of the bead synthesis process. The results of this study are presented in Figure 9. The rates achieved in the media batch reactors were very similar to those obtained with GG beads that were synthesized 6 months earlier. The rate estimates are provided in Figure S18. These results illustrate the ability to reproducibly synthesis the GG beads co-encapsulated with TBOS and strain ATCC 21198. The long-term effectiveness was also reproduced when results in media (Figure S17) are compared with those presented in Figure 4. Acetylene treated controls in these batch reactors with beads, not included tests presented in Figure 4, show similar rates of O_2 uptake as non-treated reactors, consistent with the SCAM not needed for alcohol utilization. Acetylene, however, effectively inhibited the cometabolic transformation of *cis*-DCE, 1,1,1-TCA, and 1,4-D. Both the acetylene treated and the poisoned controls also show *cis*-DCE and 1,1,1-TCA were not strongly sorbed into the GG beads.

Initial rates in the groundwater/sediment microcosms were similar for all three contaminants to those obtained in media. Some slowing in the first-order rate was observed in the groundwater/sediment microcosms in the second and third additions of *cis*-DCE and 1,1,1-TCA. The single addition of 1,4-D was reduced by 2 orders of magnitude in the media batch reactors and one in the GW/sediment microcosms. Oxygen consumption rates were similar in the media and GW/sediment microcosm. The media and GW/sediments were operated for 220 days with repetitive additions of the three contaminants. Oxygen was also added when needed. The results of the long-term incubation are shown in Figure S17. Effective long-

term treatment was achieved in both the media and the GW/sediment microcosms. The first-order rate estimates presented in Figure S18, shows the rate of 1,1,1-TCA in the second addition being about a factor of three lower in the microcosm compared to the media control, while the rate of *cis*-DCE in the microcosm was about a factor of four lower in the third addition. The additions of the contaminants at 205 days were rapidly removed in the media reactors. While slower rates were achieved in the GW/sediment microcosm, the three contaminants were removed over a period of approximately 15 days. Over two orders of magnitude reduction in 1,4-D was achieved. The results show that the GG beaded technology promoted effective cometabolic transformation in a GW/sediment microcosm for over 200 days of incubation.

4.0 Discussion

A long-term, passive cometabolic transformation process was developed by co-encapsulating SRCs and an axenic bacterial culture in a GG hydrogel. TBOS or T_2BOS served as SRCs that hydrolyzed at different rates to produce 1-butanol and 2-butanol respectively. The GG method generated more durable beads due to both thermal and ionic cross linking. Deterioration of alginate beads was observed in the hydrolysis tests and microbially active alginate bead tests not reported here. Abiotic rates of hydrolysis of TBOS and T_2BOS measured in solution and in both alginate and GG hydrogels, showed the rates of hydrolysis were 4 to 10 times slower in the hydrogels, with TBOS hydrolyzing at a rate 27 times faster than T_2BOS. GG was selected from long-term tests since it was more durable than alginate. More detailed studies are needed to determine the factors and mechanisms affecting the rates of hydrolysis of TBOS and T_2BOS and other orthosilcates in hydrogels.

Isobutane-utilization activity tests demonstrated that upon encapsulation in either alginate or GG, cells of strain ATCC 21198 maintained high rates of activity. Long-term (300 day) incubation of co-encapsulated beads showed continued metabolism of the alcohols produced in the beads as indicated by O_2 consumption and CO_2 production. The rates of O_2 consumption were consistent with those expected from the abiotic rates of hydrolysis. Mass balances indicated that enzymatic hydrolysis may have occurred, consistent with observations of Vancheeswaran et al.(1999).[40] Much higher rates of O_2 consumption were observed when TBOS was co-encapsulated compared to T_2BOS. Sustained by the alcohols produced, strain ATCC 21198 was able to cometabolize mixtures of 1,1,1-TCA, *cis*-DCE, and 1,4-D that diffused from the bulk solution into the beads. Prior work of Murnane (2018)[55] showed that when grown on these SRCs, strain ATCC 21198 can cometabolize mixtures of 1,1,1-TCA and 1,4-D, and that acetylene, a frequent inhibitor of monooxygenase enzymes, inhibited the cometabolic oxidation of 1,1,1-TCA and 1,4-D, but did not block alcohol utilization. Similar observations are presented in Figure 9 with GG beads. Taken together, these results indicated that continuous cell growth and maintenance could be achieved by the slow hydrolysis of the SRCs while achieving continuous cometabolic transformation.

The underlying biochemical basis for the effects of the alcohols released from the SRCs on strain ATCC 21198 is currently unclear. One effect appears to include a direct inducing effect of these alcohols on the expression and activity of one or both of the gaseous hydrocarbon and contaminant-oxidizing monooxygenases encoded in the genome of this bacterium. These two enzymes are a propane monooxygenase (PrMO) and another soluble di-iron monooxygenase, short chain alkane monooxygenase (SCAM). An inducing effect on oxygenase expression would be compatible with the various previous reports summarized in the Introduction, of cometabolic contaminant degradation reactions catalyzed by alcohol rather than alkane-grown bacteria, including strain ATCC 21198. Another possibility is that the expression of these monooxygenases also involves a response to carbon limitation or starvation conditions. It is a common response of bacteria under carbon-limited conditions to express multiple enzyme systems and catabolic pathways so they can scavenge and benefit from trace amounts of diverse carbon sources.[56] In the case of *Rhodococcus jostii* RHA1, this starvation response includes highly elevated expression of PrMO.[57] While it may seem counterintuitive that cells may be carbon-limited when they are co-encapsulated with SRCs, certainly in the case of strain ATCC 21198 co-encapsulated with T_2BOS, measured signatures of cellular activity such as O_2 uptake and CO_2 production (Figure 5) suggest the rate of SRC hydrolysis is very slow. In the case of T_2BOS, it may be that the rate of 2-butanol release from abiotic T_2BOS hydrolysis is sufficiently rapid for the cells to maintain low levels of "maintenance metabolism" for extended periods of time, and yet sufficiently slow that the cells consume 2-butanol as fast as it is released from T_2BOS and are therefore effectively existing under carbon-limited conditions. Although we cannot exclude the possibility that there are direct effects on monooxygenase expression and activity arising from the encapsulation process itself, or the from the interactions of the cells with high concentrations of SRC within the beads, the possibility that the cells are carbon-limited in T_2BOS co-encapsulated beads is certainly supported by the observation that 2-butanol concentrations are near detection limits in the bulk solution (Figure 5F).

Irrespective of the mechanism by which SRCs sustained cometabolically active microorganisms in the co-encapsulated systems described in this study, this co-encapsulation system offers several potential advantages over conventional approaches to aerobic cometabolism. For example, an inhibitory effect of growth substrate on contaminant transformation is frequently observed in cometabolic systems in both laboratory and field studies, and this is due to competitive interactions between two or more substrates for the same oxygenase enzyme.[58–60] When cometabolism is applied for bioremediation, one reason for alternate pulsing of the electron acceptor (O_2) and growth substrates such as methane or toluene, is to lessen this competitive interaction.[59,61,62] In the system developed here, competitive inhibition is avoided since the growth substrates and contaminants are not oxidized by the same enzyme. Evidence for a consistent cometabolic transformation process that is unhindered by a variable competitive interaction, was provided

by the repeated transformation of the 1,1,1-TCA, *cis*-DCE, and 1,4-D in the batch reactors and the consistent fit of the temporal data to a first-order transformation model.

While using SRCs such as TBOS and T_2BOS avoids inhibitor competitive interactions, these compounds still enable the process of contaminant degradation and energy-generating metabolism to be decoupled. The decoupling of these two processes is fundamental to the ability of cometabolic processes to degrade contaminants to very low concentrations. For example, the ability to treat contaminants such as 1,4-D, which may have action level of 0.35 µg/L, is not practical with 1,4-D-metabolizing strains such as *Pseudonocardia dioxanivorans* CB1190 which use this compound as a sole source of carbon and energy.[63] In contrast, the log-plots shown in Figure 7 show strain ATCC 21198 co-encapsulated with SRCs in GG beads are very capable of degrading 1,4-D to such low levels, and similar two to three orders of magnitude decreases in concentrations were also observed for 1,1,1-TCA and *cis*-DCE.

Another advantage of adding co-encapsulated bacteria with SRCs is that a much lower supply of oxygen would be required, especially when T_2BOS is used as a SRC. The rate of O_2 consumption in the CET_2 reactors containing beads co-encapsulated with T_2BOS was a factor of 50 lower that the CET reactors with TBOS beads. The transformation rates, however, in the CET_2 reactors were only a factor of three lower early on and were nearly the same later. Thus, T_2BOS is a more efficient SRC with much lower rates of oxygen consumption while maintaining reasonable rates of contaminant transformation.

A final advantage of encapsulating a pure microbial culture within the hydrogel is that this approach not only represents a mechanism for highly selective and long-lived bioaugmentation, it also maximizes the amount of substrate directed to the desired, cometabolically active strain (or strains). For example, if SRCs were added directly to a contaminated aquifer without a co-encapsulated bacterium, competition for the resulting hydrolysis products would exist between diverse native microorganisms. Unless the hydrolysis product itself was highly selective for supporting the growth of cometabolically-active microorganisms, it is likely that growth of non-cometabolically active microorganisms would be promoted and the efficiency of the SRCs would be very limited. This type of population bias towards non-cometabolically active microorganisms would also be further amplified if the biostimulated cometabolically active microorganisms also suffered any toxicity effects arising from the oxidation of non-growth supporting substrates such as CAHs. Other advantages of the co-encapsulation approach include the possibility of including more than one microbial strain in a bead and the possibility of using a specific microorganism or microorganisms with cometabolic activities and oxygenase enzymes that are selected specifically to address site-specific suites of contaminants.

The batch reactor tests were performed with a very low mass of beads (2 g) per 100 ml of solution. When the mass of beads was doubled the first-order rate of 1,4-D transformation increased by a factor of

1.45. Thus, increasing the density of the bead packing would greatly enhance the rates of transformation. An estimate can be made of the potential rates if the co-encapsulated beads were densely packed to make a continuous flow column representative of a permeable reactive barrier. Assuming a porosity of 0.40 and a bead density approximately equal to 1 g/mL, the rate of reaction would be increased approximately 30-fold compared to the rates estimated in the batch reactors. The first-order rate determined in the batch reactor for TBOS of 0.15 day^{-1} (Figure 6) would scale to 4.5 day^{-1} in a packed bed configuration. The residence time required to achieve 99% transformation of the 1,4-D would be approximately 1 day. Using the slower rate determined with long-term incubation of 0.03 day^{-1} would yield a rate coefficient of 0.9 day^{-1} in a packed bed, which would require a 5-day residence time to achieve 99% transformation of 1,4-D. There are many factors that would influence these estimates. The contaminant concentrations 250 µg/L were low, which resulted in a reasonable first-order fit to the data. As concentrations increase, a first-order approximation would likely not apply. Also, transformation toxicity and transformation yields would become important. With the higher packing density, the rates of oxygen consumption would increase and a supply O_2 would be required. Studies are currently being conducted in densely packed columns to demonstrate that short residence times would be required to achieve very high extents of treatment. Detailed modeling studies are needed that incorporate mass transfer, hydrolysis, microbial process of growth and decay along with the complex process of cometabolism in order to better understand the results observed here and to simulate continuous flow experiments, such as packed columns. Modeling, for example, may help determine what factors contributed to the slowing in the rates of cometabolic transformation over the course of the batch incubations.

The range of contaminants transformed is the same as those observed when strain ATCC 21198 was grown on isobutane [17,18]. VC and 1,1-DCE were transformed in the later stage of the batch tests. Based on resting cell studies with strain ATCC 21198 grown on isobutane, 1,2-DCA, 1,1-DCA and 1,2,3-trichloropropane could also be treated by both TBOS and T_2BOS co-encapsulated GG beads. The potential mixture of 1,1-DCE and 1,1-DCA, both abiotic and biotic transformation products of 1,1,1-TCA, respectively, along with 1,4-D could be treated by the GG beads that were tested. The co-encapsulated beads that were created would also be able to treat *cis*-DCE and VC, which are the products of the reductive dehalogenation of TCE.

For subsurface in-situ treatment, O_2 addition would likely be required. Oxygen could be added via air sparing or hydrogen peroxide addition. To create a completely passive system, solid slow release compounds that produce O_2[64,65] could be used along with the GG bead system. Studies are needed to develop completely passive cometabolic systems using oxygen release compounds and the co-encapsulated bead technology presented here. In addition to subsurface systems, the co-encapsulated bead technology that

was developed might also be used for ex-situ treatment of CAHs and 1,4-D in packed columns or fluidized bed reactors.

The structural stability of the hydrogel beads is important if long-term treatment is to be achieved. Figure S16 shows the CET reactors and the CET_2 reactors after 232 days of incubation on a shaker table at 100 rpm. As previously discussed, much higher rates of metabolism occurred in the CET reactors as a result of the higher rates of hydrolysis of TBOS compared to T_2BOS. The beads floating on top in the CET reactors (left) are orange in color that is associated with the higher biomass that developed. CET_2 reactors (right) co-encapsulated with T_2BOS have much lower metabolic activity resulting in lower biomass growth and are clearer in color. Also, there is a higher optical density in CET reactors, which is associated with deterioration of the beads as a result of continuous agitation and microbial growth in the beads. CET_2 reactors are much clearer, showing the beads remain intact even after an incubation of 232 days on the shaker table.

5.0. Conclusions

A method was developed to co-encapsulate strain ATCC 21198 in GG hydrogel beads with the organosilicates TBOS and T_2BOS that slowly hydrolyze to produce 1-butanol and 2-butanol, respectively. Strain ATCC 21198 in the beads was able to continuously cometabolize a mixture of 1,1,1-TCA, *cis*-DCE and 1,4-D for over 300 days, and successive additions of a contaminant mixture were transformed. Rates of O_2 utilization and CO_2 production were much higher in batch reactors with beads containing TBOS compared to T_2BOS, which was consistent with its much greater rate of abiotic hydrolysis. Reaction rates decreased with prolonged incubation, but slowed to a lesser extent with beads containing T_2BOS. Appropriately scaled first-order rates indicate very high extents of contaminant transformation could be achieved with a residence time of a few days if co-encapsulated beads were densely packed in a permeable reactive barrier. Studies in groundwater/sediment microcosms also demonstrated that long-term cometabolic treatment can be achieved under conditions that mimic the subsurface. Based on the lower rate of oxygen consumption while achieving similar long-term rates, T_2BOS is a much more effective substrate than TBOS to co-encapsulate with strain ATCC 21198.

Conflict of Interest Statement

There are no conflicts to declare.

Acknowledgments

This study was funded by the US Department of Defense Strategic Environmental Research and Development Program (SERDP), Grant ER-2716. The authors thank Mohammad Azizian for his support of the analytical methods and Christy Smith for her support of microbiological methods.

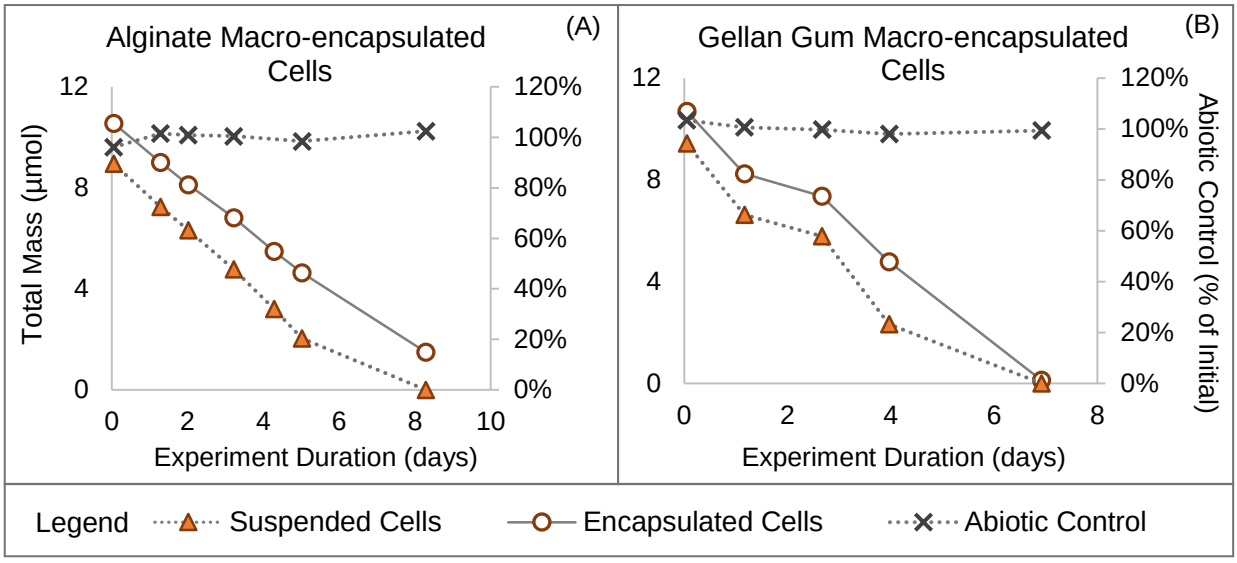

Figure 1. Isobutane utilization curves measured for strain ATCC 21198 suspended and encapsulated in (A) spherical alginate macro-beads ~2mm in diameter, (B) cylindrical GG macro-beads (~2 mm x 2 mm) and, (C) spherical GG micro-beads (~10-100 µm) in diameter. All data points are averages of duplicate reactors.

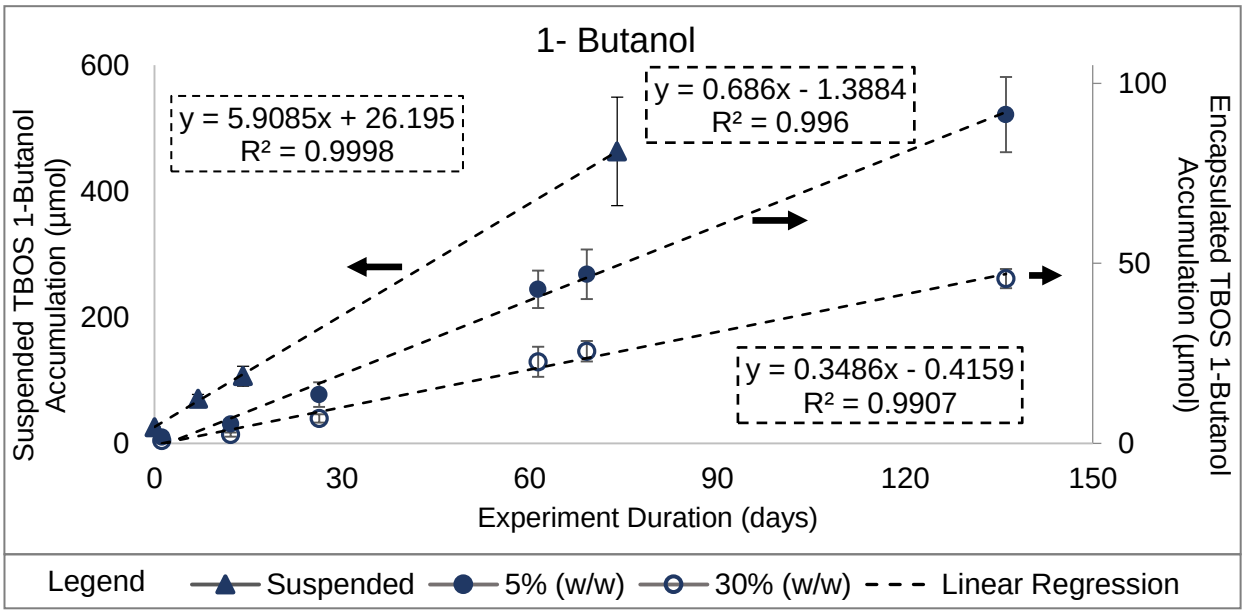

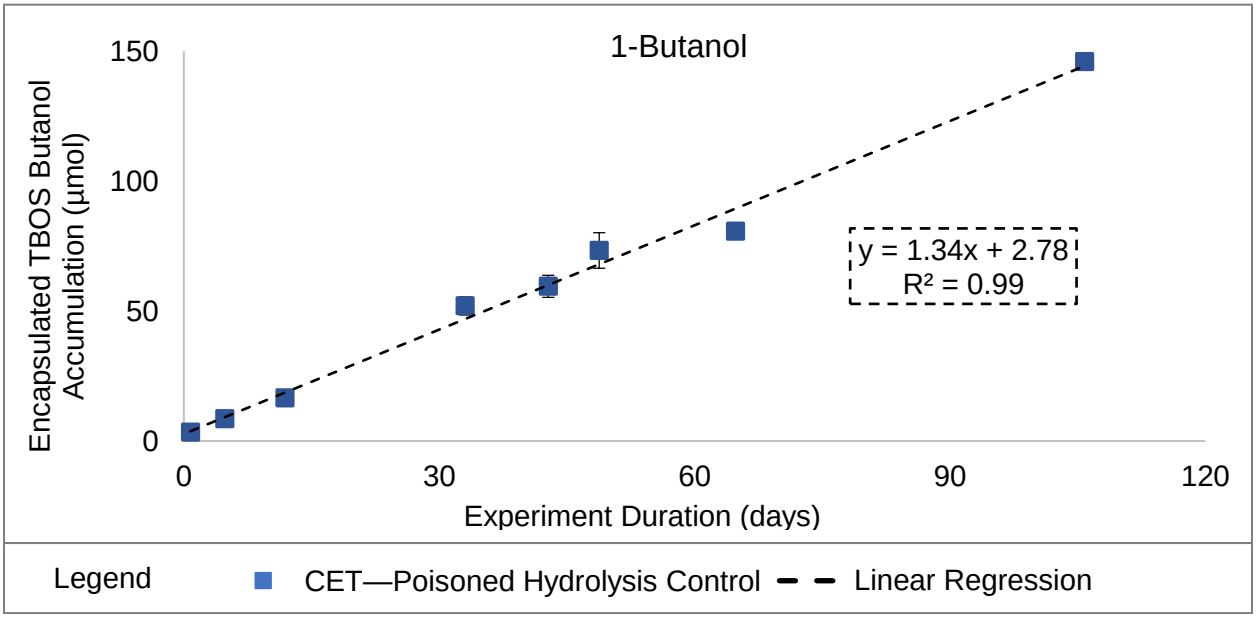

Figure 2. (Top) Measured 1-butanol masses in solution from the abiotic hydrolysis of suspended (left-axis) and alginate encapsulated TBOS (right-axis). Total TBOS solution concentrations of 1000 mg/L and bead mass loading 5 and 30% (wt/wt). Excel linear trend-line functions are fit to the time-series and black-dashed boxes represent linear regression. Data points are averages between duplicate (suspended) or triplicate (encapsulated) reactors for each treatment, and errors bars are the range of duplicates or 95% confidence intervals for triplicates. (Bottom) Measured 1-butanol masses in solution from the abiotic hydrolysis of duplicate GG encapsulated TBOS. Total TBOS solution concentration of 1500 mg/L and bead mass loading 8% (wt/wt). Error bars are range of the duplicates.

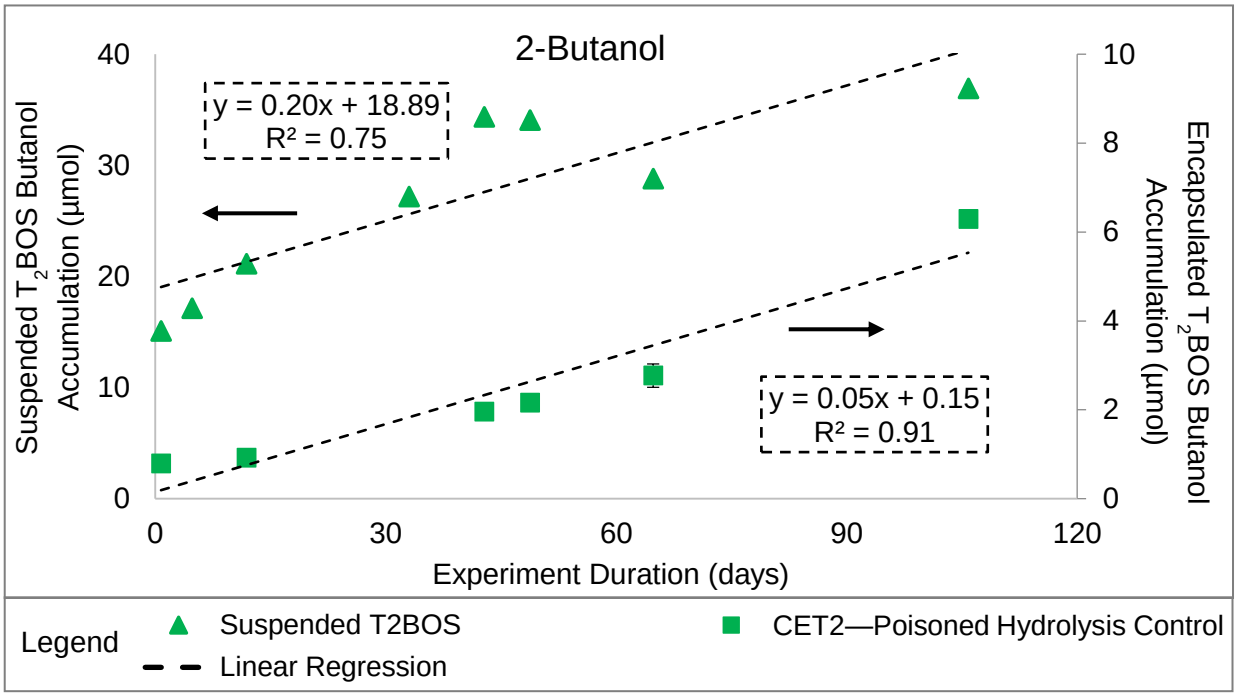

Figure 3. Measured 2-butanol masses in solution from the abiotic hydrolysis of suspended (left-axis) and GG encapsulated T_2BOS (right-axis). Total T_2BOS solution concentrations of 1500 mg/L and bead mass loading 8% (wt/wt). Black arrows signify the axis that time-series correspond to. Excel linear trend-line functions fit to time-series and the black-dashed boxes represent linear regression equations calculated by excel linear trend-line tool. Data are averages between duplicate reactors in each treatment and errors bars are the range of the duplicates.

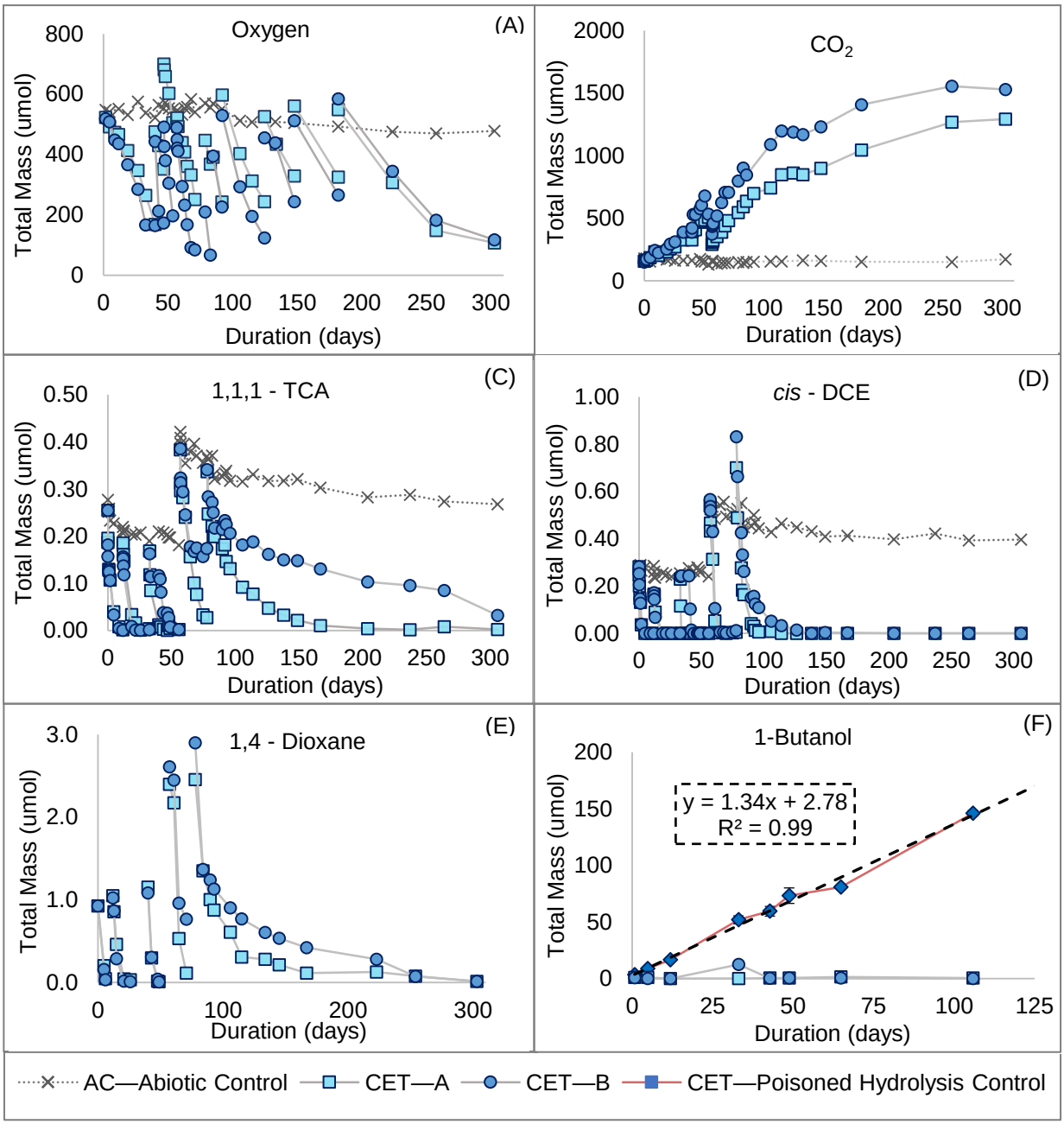

Figure 4. Longevity study of the cometabolism of 1,1,1-TCA, *cis*-DCE and 1,4-D in batch CET reactors containing co-encapsulated GG beads with TBOS and strain ATCC 21198. (A-B) O_2 and CO_2 respiration data. (C-E) Contaminant transformation data. (F) 1-butanol production data in sodium azide (2% w/v) poisoned hydrolysis control and live reactors. (AC) – Abiotic control. (CET) Strain ATCC 21198 co-encapsulated with 8% (wt/wt) TBOS. Alphabetical designations CET-A and CET-B are for replicate live reactors. AC has a single reactor. The total mass was determined using Henry's Law (Equation 1). O_2 masses of ~ 180 µmol are assumed to represent anoxic conditions. Breaks in the time-series signify successive additions of O_2 and the contaminants.

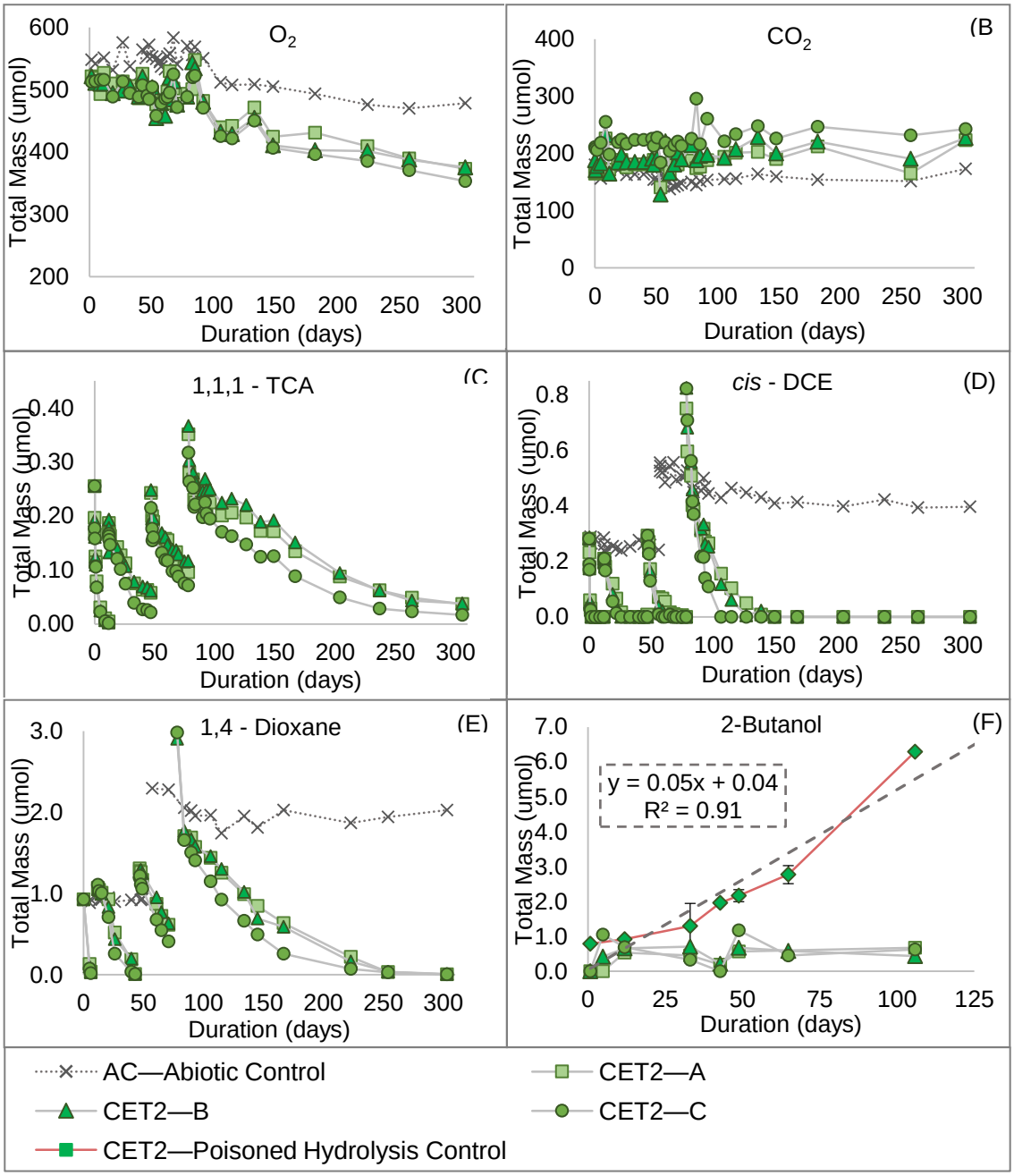

Figure 5. Longevity study of the cometabolism of 1,1,1-TCA, *cis*-DCE and 1,4-D in batch CET_2 reactors containing co-encapsulated GG beads with T_2BOS and ATCC 21198. (A-B) O_2 and CO_2 respiration data. (C-E) Contaminant transformation data. (F) 1-butanol production data in sodium azide (2% w/v) poisoned hydrolysis control and live reactors. (AC) – Abiotic control. (CET_2) ATCC 21198 co-encapsulated with 8% (wt/wt) TBOS. Alphabetical designations CET_2-A, CET_2-B, CET_2-C are for triplicate live reactors. AC has a single reactor. The total mass was determined using Henry's Law (Equation 1). Breaks in the time-series signify successive additions of O_2 and the contaminants.

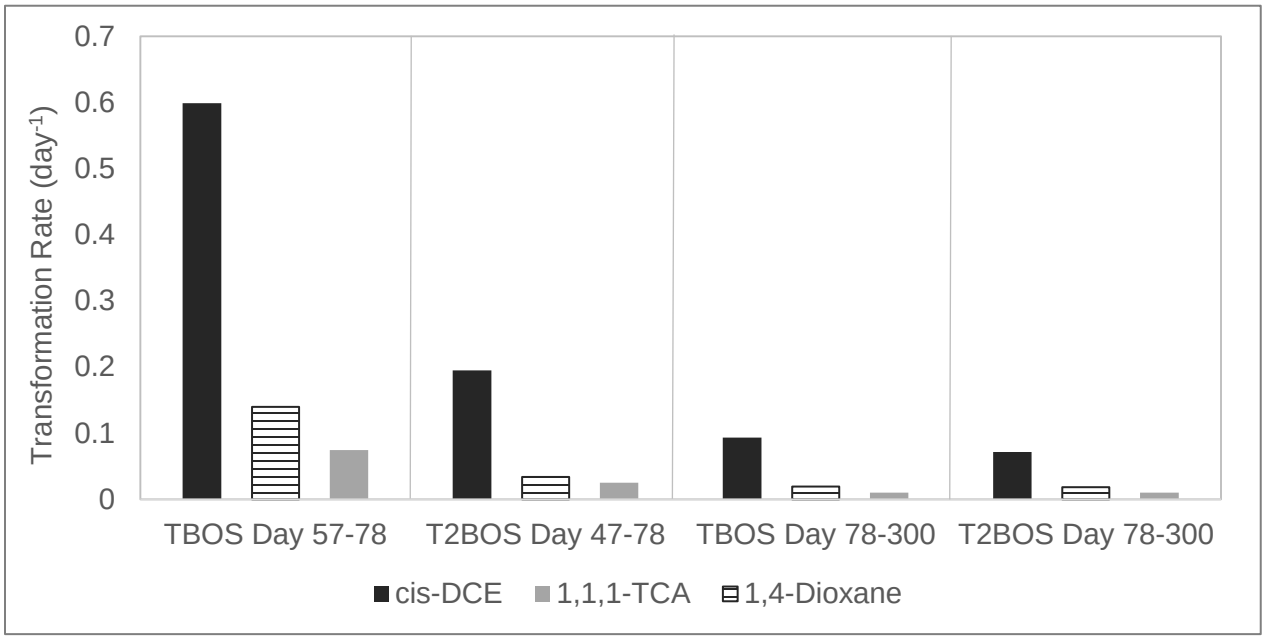

Figure 6. First-order transformation rates for successive transformations of 1,1,1-TCA, *cis*-DCE, and 1,4-D. The first-order plots are provided in Figure S10-S15 in the Supplementary Information.

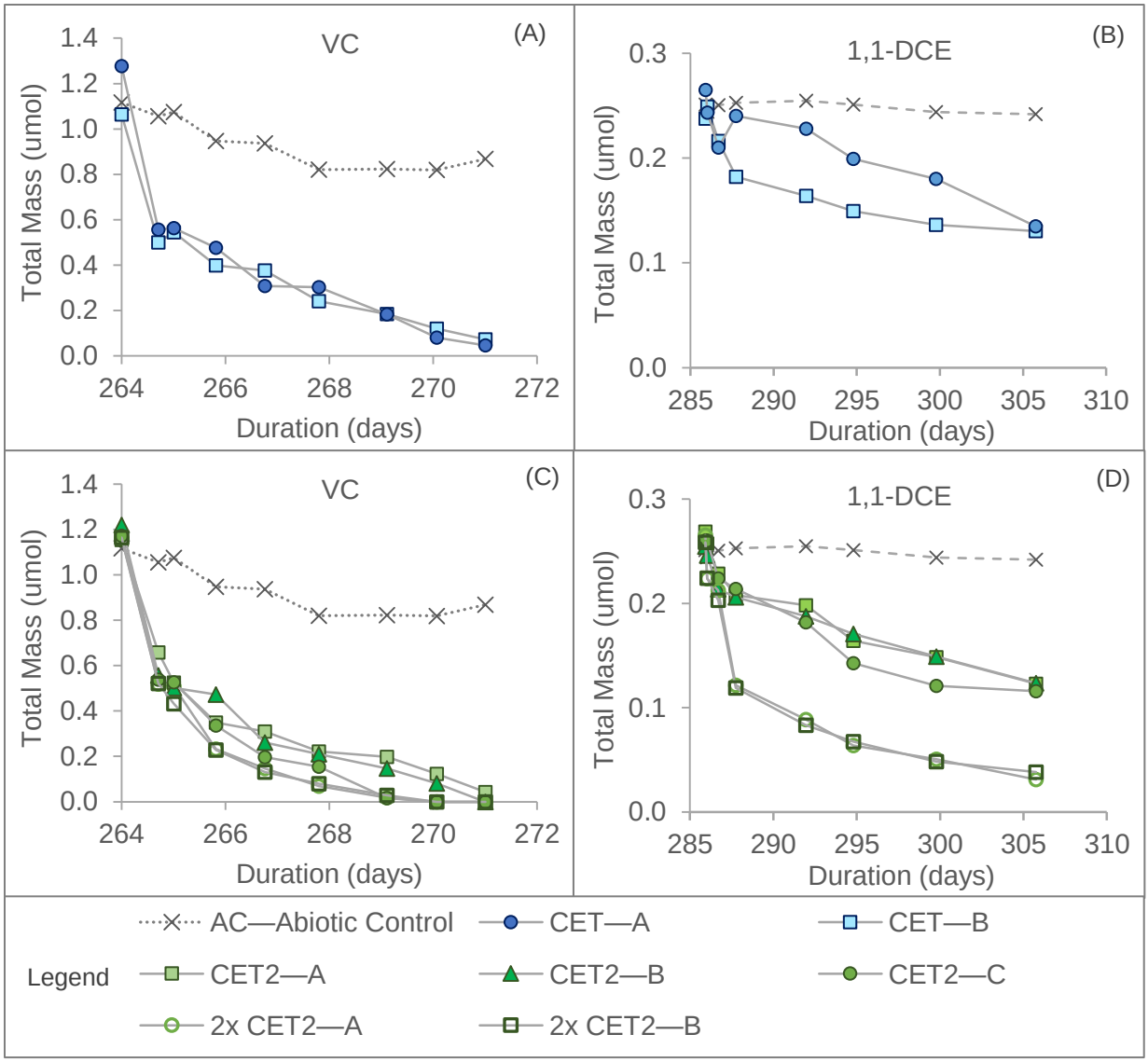

Figure 7. VC (A, C) and 1,1-DCE (B, D) Cometabolic transformation with TBOS and T_2BOS co-encapsulated with cells of strain 21198 after long-term (264 day) exposure to *cis*-DCE, 1,1,1-TCA, and 1,4D. (AC) - Abiotic control. (CET) - Cells co-encapsulated with 8% (wt/wt) TBOS. (CET_2) - Cells co-encapsulated with 8% (wt/wt) T_2BOS. (2X CET_2) addition of twice the mass of co-encapsulated beads (4 g) with 8% (wt/wt) T_2BOS.

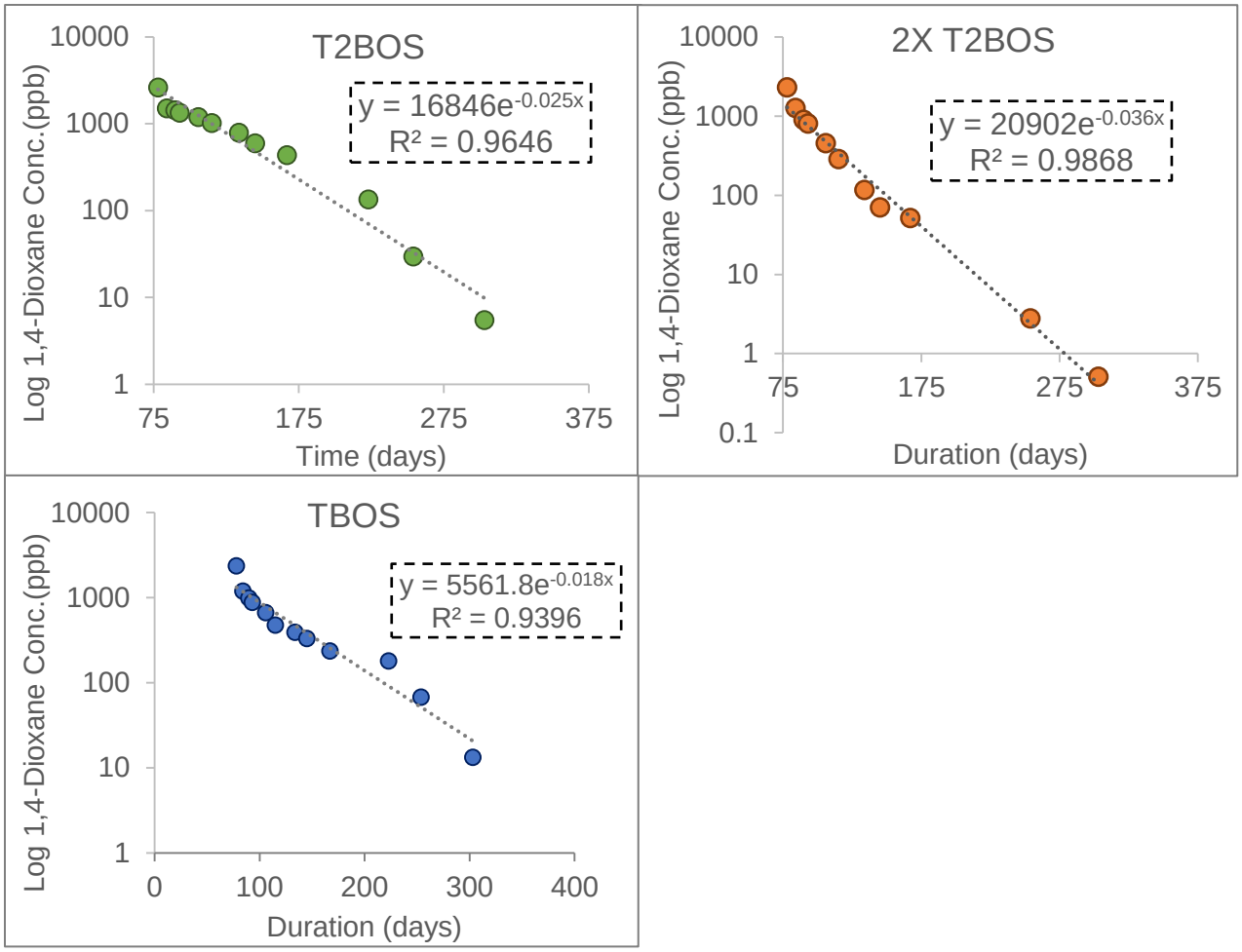

Figure 8. Long-term first-order transformation of the last addition of 1,4-D to the CET (TBOS/21198) and CET_2 (T_2BOS/21198) batch reactors (1X beads) shown in Figures 4 and 5. The 2X bead results are for a batch reactor that has 2 times the amount of GG beads as the CET_2 (1X) reactors.

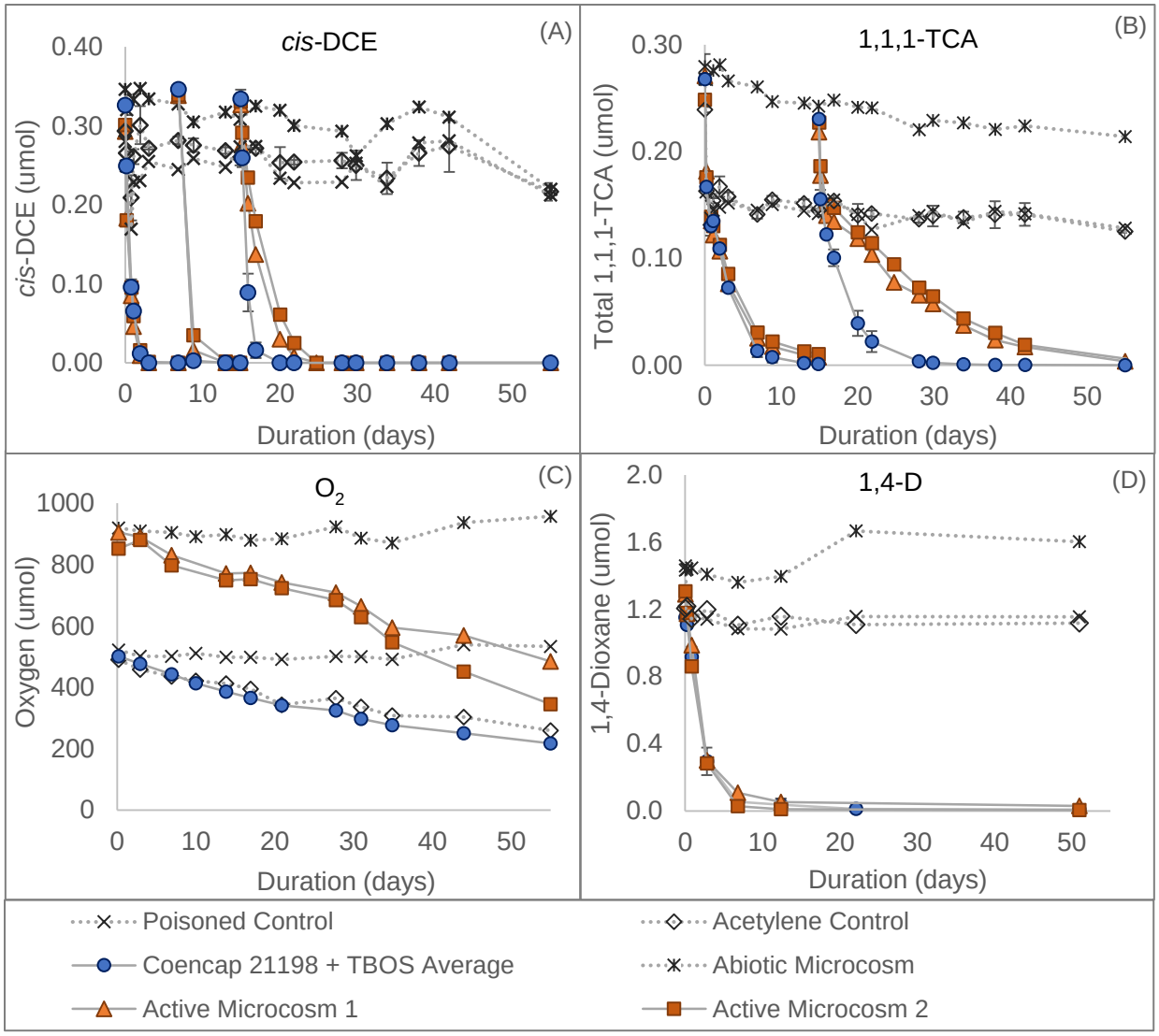

Figure 9. Comparison of co-encapsulated TBOS and strain ATCC 21198 GG beads in batch reactors with media and groundwater/ aquifer solid microcosms. (A) *cis*-DCE; B (1,1,1-TCA); (C) O_2; (D) 1,4-D. The media reactors replicate the conditions of the tests presented in Figure 4, with GG beads synthesized six months after those tests.

I. References

1. Squillace PJ, Scott JC, Moran MJ, Nolan BT, Kolpin DW. VOCs, Pesticides, Nitrate, and Their Mixtures in Groundwater Used for Drinking Water in the United States. *Environ Sci Technol*. 2002;36(9):1923-1930. doi:10.1021/es015591n

2. Zogorski JS, ed. Volatile organic compounds in the nation's ground water and drinking-water supply wells. 2006.

3. NIOSH. CDC - Organic Solvents - NIOSH Workplace Safety and Health Topic. https://www.cdc.gov/niosh/topics/organsolv/default.html. Published 2013. Accessed August 8, 2018.

4. US EPA O of L and EM. Technical Fact Sheet - 1,4-Dioxane. November 2017. https://www.epa.gov/sites/production/files/2014-03/documents/ffrro_factsheet_contaminant_14-dioxane_january2014_final.pdf. Accessed June 26, 2018.

5. Mohr T. Solvent Stabilizers. *Santa Clara Valley Water District*. 2001.

6. Adamson DT, McGuire TM, Newell CJ, Stroo H. Sustained treatment: Implications for treatment timescales associated with source-depletion technologies. *Remediation*. 2011;21(2):27-50. doi:10.1002/rem.20280

7. DeRosa CT, Wilbur S, Holler J, Richter P, Stevens Y-W. Health Evaluation of 1,4-Dioxane. *Toxicology and Industrial Health*. 1996;12(1).

8. Adamson DT, Mahendra S, Walker KL, Rauch SR, Sengupta S, Newell CJ. A Multisite Survey To Identify the Scale of the 1,4-Dioxane Problem at Contaminated Groundwater Sites. *Environ Sci Technol Lett*. 2014;1(5):254-258. doi:10.1021/ez500092u

9. Liu C, Ball W. Back diffusion of chlorinated solvent contaminants from a Natural Aquitard to Remediated Aquifer Under Well-Controlled Field Conditions: Predictions and Measurements. *Groundwater*. 2001;40.2:175-184.

10. Parker BL, Chapman SW, Guilbeault MA. Plume persistence caused by back diffusion from thin clay layers in a sand aquifer following TCE source-zone hydraulic isolation. *Journal of Contaminant Hydrology*. 2008;102(1-2):86-104. doi:10.1016/j.jconhyd.2008.07.003

11. McElroy AC, Hyman MR, Knappe DRU. 1,4-Dioxane in drinking water: emerging for 40 years and still unregulated. *Current Opinion in Environmental Science & Health*. 2019;7:117-125. doi:10.1016/j.coesh.2019.01.003

12. Mohr TKG. Environmental Investigation and Remediation: 1,4-Dioxane and other Solvent Stabilizers. CRC Press. https://www.crcpress.com/Environmental-Investigation-and-

Remediation-14-Dioxane-and-other-Solvent/Mohr-Stickney-DiGuiseppi/p/book/9781566706629. Published March 25, 2010. Accessed August 8, 2018.

13. Semprini L. Strategies for the aerobic co-metabolism of chlorinated solvents. *Current Opinion in Biotechnology*. 1997;8(3):296-308. doi:10.1016/S0958-1669(97)80007-9

14. Semprini L. In situ bioremediation of chlorinated solvents. *Environ Health Perspect*. 1995;103(Suppl 5):101-105.

15. Hand S, Wang B, Chu K-H. Biodegradation of 1,4-dioxane: Effects of enzyme inducers and trichloroethylene. *Science of The Total Environment*. 2015;520:154-159. doi:10.1016/j.scitotenv.2015.03.031

16. Frascari D, Zanaroli G, Danko AS. In situ aerobic cometabolism of chlorinated solvents: A review. *Journal of Hazardous Materials*. 2015;283:382-399. doi:10.1016/j.jhazmat.2014.09.041

17. Rich S. Kinetic Analysis of the Aerobic Degradation of Chlorinated Ethenes by the Mycobacterium ELW-1 and Chlorinated Ethanes and Ethenes by Rhodococcus rhodochrous ATCC®21198™. *Oregon State University, Honors College Thesis*. 2015.

18. Krippaehne JK. Cometabolism of 1,4-Dioxane and Chlorinated Aliphatic Hydrocarbons by Pure Cultures of Rhodococcus rhodochrous 21198 and Mycobacterium ELW1 and in Groundwater Microcosms Fed Isobutane and Isobutene as Growth Substrates. *Oregon State University, MS Thesis*. 2018.

19. Rolston HM, Hyman MR, Semprini L. Aerobic cometabolism of 1,4-dioxane by isobutane-utilizing microorganisms including Rhodococcus rhodochrous strain 21198 in aquifer microcosms: Experimental and modeling study. *Science of The Total Environment*. 2019;694:133688. doi:10.1016/j.scitotenv.2019.133688

20. Lippincott D, Streger SH, Schaefer CE, Hinkle J, Stormo J, Steffan RJ. Bioaugmentation and Propane Biosparging for In Situ Biodegradation of 1,4-Dioxane. *Groundwater Monit R*. 2015;35(2):81-92. doi:10.1111/gwmr.12093

21. Chu M-YJ, Bennett PJ, Dolan ME, et al. Concurrent Treatment of 1,4-Dioxane and Chlorinated Aliphatics in a Groundwater Recirculation System Via Aerobic Cometabolism. *Groundwater Monit R*. 2018;38(3):53-64. doi:10.1111/gwmr.12293

22. Azizian MF, Istok JD, Semprini L. Evaluation of the in-situ aerobic cometabolism of chlorinated ethenes by toluene-utilizing microorganisms using push–pull tests. *Journal of Contaminant Hydrology*. 2007;90(1-2):105-124. doi:10.1016/j.jconhyd.2006.09.015

23. Connon SA, Tovanabootr A, Dolan M, Vergin K, Giovannoni SJ, Semprini L. Bacterial community composition determined by culture-independent and -dependent methods during propane-stimulated bioremediation in trichloroethene-contaminated groundwater. *Environmental Microbiology*. 2005;7(2):165-178. doi:10.1111/j.1462-2920.2004.00680.x

24. Scherer MM, Richter S, Valentine RL, Alvarez PJJ. Chemistry and Microbiology of Permeable Reactive Barriers for *In Situ* Groundwater Clean up. *Critical Reviews in Microbiology*. 2000;26(4):221-264. doi:10.1080/10408410091154237

25. Upadhyay S, Sinha A. Role of Microorganisms in Permeable Reactive Bio-Barriers (PRBBs) for Environmental Clean-Up: A Review. *Global NEST Journal*. 2018;20(2):269-280. doi:10.30955/gnj.002525

26. Moslemy P, Neufeld RJ, Guiot SR. Biodegradation of gasoline by gellan gum-encapsulated bacterial cells. *Biotechnology and Bioengineering*. 2002;80(2):175-184. doi:10.1002/bit.10358

27. Petrich CR, Stormo KE, Ralston DR, Crawford RL. Encapsulated Cell Bioremediation: Evaluation on the Basis of Particle Tracer Tests. *Groundwater*. 1998;36(5):771-778. doi:10.1111/j.1745-6584.1998.tb02194.x

28. Cassidy MB, Lee H, Trevors JT. Environmental applications of immobilized microbial cells: A review. *Journal of Industrial Microbiology*. 1996;16(2):79-101. doi:10.1007/BF01570068

29. Moslemy P, Neufeld RJ, Millette D, Guiot SR. Transport of gellan gum microbeads through sand: an experimental evaluation for encapsulated cell bioaugmentation. *Journal of Environmental Management*. 2003;69(3):249-259. doi:10.1016/j.jenvman.2003.09.003

30. Chen Y-M, Lin T-F, Huang C, Lin J-C, Hsieh F-M. Degradation of phenol and TCE using suspended and chitosan-bead immobilized Pseudomonas putida. *Journal of Hazardous Materials*. 2007;148(3):660-670. doi:10.1016/j.jhazmat.2007.03.030

31. Doner LW, Bécard G. Solubilization of gellan gels by chelation of cations. *Biotechnol Tech*. 1991;5(1):25-28. doi:10.1007/BF00152749

32. Osmalek T, Froelich A, Tasarek S. Application of gellan gum in pharmacy and medicine. *International Journal of Pharmaceutics*. 2014;466(1-2):328-340.

33. Norton S. Gellan gum gel as entrapment matrix for high temperature fermentation processes: A rheological study. *Biotechnology Techniques*. 1990;4.5:351-356.

34. Grasdalen H, Smidsrod O. Gelation of gellan gum. *Carbohydrate Polymers*. 1987;7(5):371-393.

35. Camelin I, Lacroix C, Paquin C, Prevost H, Cachon R, Divies C. Effect of chelatants on gellan gel rheological properties and setting temperature for immobilization of living bifidobacteria. *Biotechnol Prog*. 1993;9(3):291-297. doi:10.1021/bp00021a008

36. Zhang S, Mao G, Crittenden J, Liu X, Du H. Groundwater remediation from the past to the future: A bibliometric analysis. *Water Research*. 2017;119:114-125. doi:10.1016/j.watres.2017.01.029

37. Thankitkul S. Kinetic Analysis and Modeling Cometabolic Transformation of CAHs by R. Rhodochrous ATCC® 21198^{TM}. *Oregon State University, MS Thesis*. 2016.

38. Arkles B, Steinmetz JR, Zazyczny J, Mehta P. Factors contributing to the stability of alkoxysilanes in aqueous solution. *Journal of Adhesion Science and Technology*. 1992;6(1):193–206.

39. Osterholtz FD, Pohl ER. Kinetics of the hydrolysis and condensation of organofunctional alkoxysilanes: a review. *Journal of Adhesion Science and Technology*. 1992;6(1):127–149.

40. Vancheeswaran S, Halden RU, Williamson KJ, Ingle, JD, Semprini L. Abiotic and Biological Transformation of Tetraalkoxysilanes and Trichloroethene/cis -1,2-Dichloroethene Cometabolism Driven by Tetrabutoxysilane-Degrading Microorganisms. *Environmental Science & Technology*. 1999;33(7):1077-1085. doi:10.1021/es981021k

41. Semprini L, Vancheeswaran S. Slow Release Substrates for Driving Microbial Transformations of Environmental Contaminants. *US Patent No 6,472,198*. 2002.

42. Smith CA, O'Reilly KT, Hyman MR. Cometabolism of Methyl tertiary Butyl Ether and Gaseous n-Alkanes by Pseudomonas mendocina KR-1 Grown on C5 to C8 n-Alkanes. *Applied and Environmental Microbiology*. 2003;69(12):7385-7394. doi:10.1128/AEM.69.12.7385-7394.2003

43. Kuntz RL, Brown LR, Zappi ME, French WT. Isopropanol and acetone induces vinyl chloride degradation in Rhodococcus rhodochrous. *Journal of Industrial Microbiology and Biotechnology*. 2003;30(11):651-655. doi:10.1007/s10295-003-0091-8

44. Kottegoda S, Waligora E, Hyman M. Metabolism of 2-Methylpropene (Isobutylene) by the Aerobic Bacterium Mycobacterium sp. Strain ELW1. Löffler FE, ed. *Appl Environ Microbiol*. 2015;81(6):1966-1976. doi:10.1128/AEM.03103-14

45. Rice EW, Baird RB, Eaton AD, Editors. *Standard Methods for the Examination of Water and Wastewater*.; 2017.

46. Rasmussen M, Semprini L. Co-Encapsulation of Slow Release Substrates and Microbial Cultures in Alginate and Gellan Gum Beads to Promote the Co-metabolic Transformation of 1,4-Dioxane and Chlorinate Aliphatic Hydrocarbons. *Oregon State University, MS Thesis*. 2018.

47. Moslemy P, Guiot SR, Neufeld RJ. Production of size-controlled gellan gum microbeads encapsulating gasoline-degrading bacteria. *Enzyme and Microbial Technology*. 2002;30(1):10–18.

48. Tan SM, Heng PWS, Chan LW. Development of Re-Usable Yeast-Gellan Gum Micro-Bioreactors for Potential Application in Continuous Fermentation to Produce Bio-Ethanol. *Pharmaceutics*. 2011;3(4):731-744. doi:10.3390/pharmaceutics3040731

49. Hamid S, Bae W, Kim S, Amin MT. Enhancing co-metabolic degradation of trichloroethylene with toluene using *Burkholderia vietnamiensis* G4 encapsulated in polyethylene glycol polymer. *Environmental Technology*. 2014;35(12):1470-1477. doi:10.1080/09593330.2013.871045

50. Li RH, Altreuter D, Gentile F. Transport characterization of hydrogel matrices for cell encapsulation. *Biotechnology and Bioengineering*. 1996;50(4):9.

51. Draper WM, Dhoot JS, Remoy JW, Perera SK. Trace-level determination of 1,4-dioxane in water by isotopic dilution GC and GC-MS. *Analyst*. 2000;125(8):1403-1408.

52. Gosmann B, Rehm H. Oxygen uptake of microorganisms entrapped in Ca-alginate. *Appl Microbiol Biotechnol*. 1986;23(3-4). doi:10.1007/BF00261907

53. Hiemstra H, Dijkhuizen L, Harder W. Diffusion of oxygen in alginate gels related to the kinetics of methanol oxidation by immobilized Hansenula polymorpha cells. *European J Appl Microbiol Biotechnol*. 1983;18(4):189-196. doi:10.1007/BF00501507

54. Gustafsson J, KTH. Visual Minteq, Version 3.0 Compiled in Visual Basic.NET 2005. *Department of Land and Water Resources Engineering*. August 2012.

55. Murnane R. Long-Term Transformation of 1,4-Dioxane and 1,1,1-Trichloroethane by Rhodococcus rhodochrous in the Presence of Alcohol-Producing Slow-Release Compounds. *Oregon State University, MS Thesis*. 2018.

56. Egli T. How to live at very low substrate concentration. *Water Research*. 2010;44(17):4826-4837. doi:10.1016/j.watres.2010.07.023

57. Patrauchan MA, Miyazawa D, LeBlanc JC, et al. Proteomic Analysis of Survival of Rhodococcus jostii RHA1 during Carbon Starvation. *Appl Environ Microbiol*. 2012;78(18):6714-6725. doi:10.1128/AEM.01293-12

58. Criddle CS. The kinetics of cometabolism. *Biotechnol Bioeng*. 1993;41(11):1048-1056. doi:10.1002/bit.260411107

59. Semprini L, McCarty PL. Comparison Between Model Simulations and Field Results for In-Situ Biorestoration of Chlorinated Aliphatics: Part 2, Cometabolic Transformations. *Ground Water*. 1992;30.

60. Kim Y, Arp DJ, Semprini L. A combined method for determining inhibition type, kinetic parameters, and inhibition coefficients for aerobic cometabolism of 1,1,1-trichloroethane by a butane-grown mixed culture. *Biotechnol Bioeng*. 2002;77(5):564-576. doi:10.1002/bit.10145

61. McCarty PL, Goltz MN, Hopkins GD, et al. Full-Scale Evaluation of *In Situ* Cometabolic Degradation of Trichloroethylene in Groundwater through Toluene Injection. *Environ Sci Technol*. 1998;32(1):88-100. doi:10.1021/es970322b

62. Semprini L, Roberts PV, Hopkins GD, McCarty PL. A Field Evaluation of In-Situ Biodegradation of Chlorinated Ethenes: Part 2, Results of Biostimulation and Biotransformation Experiments. *Ground Water*. 1990;28(5):715-727. doi:10.1111/j.1745-6584.1990.tb01987.x

63. Mahendra S. Pseudonocardia dioxanivorans sp. nov., a novel actinomycete that grows on 1,4-dioxane. *INTERNATIONAL JOURNAL OF SYSTEMATIC AND EVOLUTIONARY MICROBIOLOGY*. 2005;55(2):593-598. doi:10.1099/ijs.0.63085-0

64. Koenigsberg SS, Sandefur CA. The Use of Oxygen Release Compound for the Accelerated Bioremediation of Aerobically Degradable Contaminants: The Advent of Time-Release Electron Acceptors. *Remediation*. 1999;10(1):3-29. doi:10.1002/rem.3440100103

65. Waite AJ, Bonner JS, Autenrieth R. Kinetics and Stoichiometry of Oxygen Release from Solid Peroxides. *Environmental Engineering Science*. 1999;16(3):187-199. doi:10.1089/ees.1999.16.187

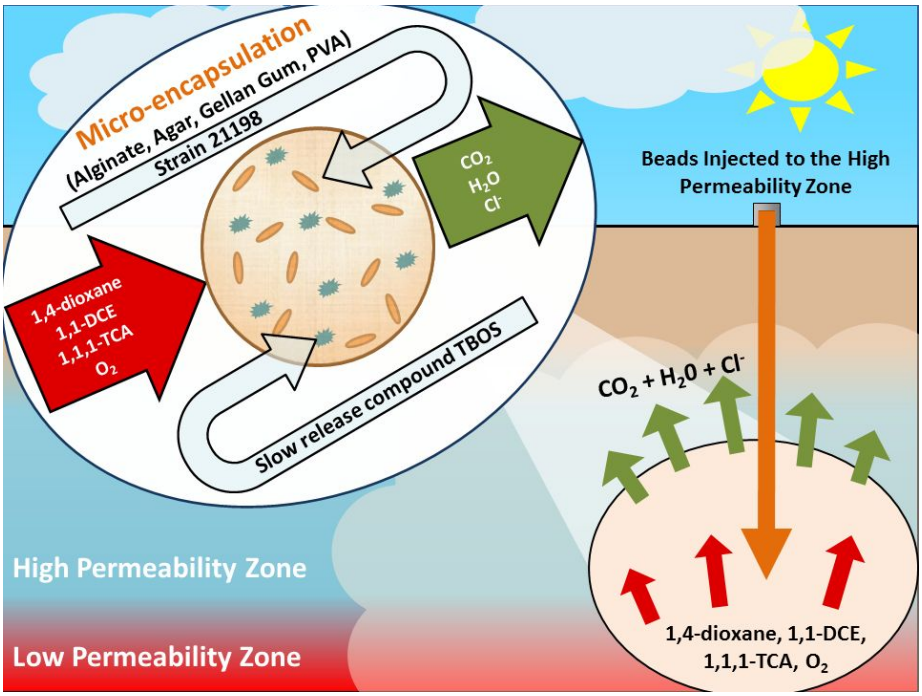
Micro-encapsulation
(Alginate, Agar, Gellan Gum, PVA)
Strain 21198
CO_2
H_2O
Cl^-
1,4-dioxane
1,1-DCE
1,1,1-TCA
O_2
Slow release compound TBOS
Beads Injected to the High Permeability Zone
$CO_2 + H_2O + Cl^-$
1,4-dioxane, 1,1-DCE, 1,1,1-TCA, O_2
High Permeability Zone
Low Permeability Zone